AD-A078 037 GEORGE WASHINGTON UNIV WASHINGTON D C DEPT OF CHEMISTRY F/G 7/2
FINAL STATE CORRELATION EFFECTS IN AUGER LINESHAPES; APPLICATIO--ETC(U)
NOV 79 D E RAMAKER N00014-78-C-0496
UNCLASSIFIED TR-1 NL

1 OF 1
ADA 078037

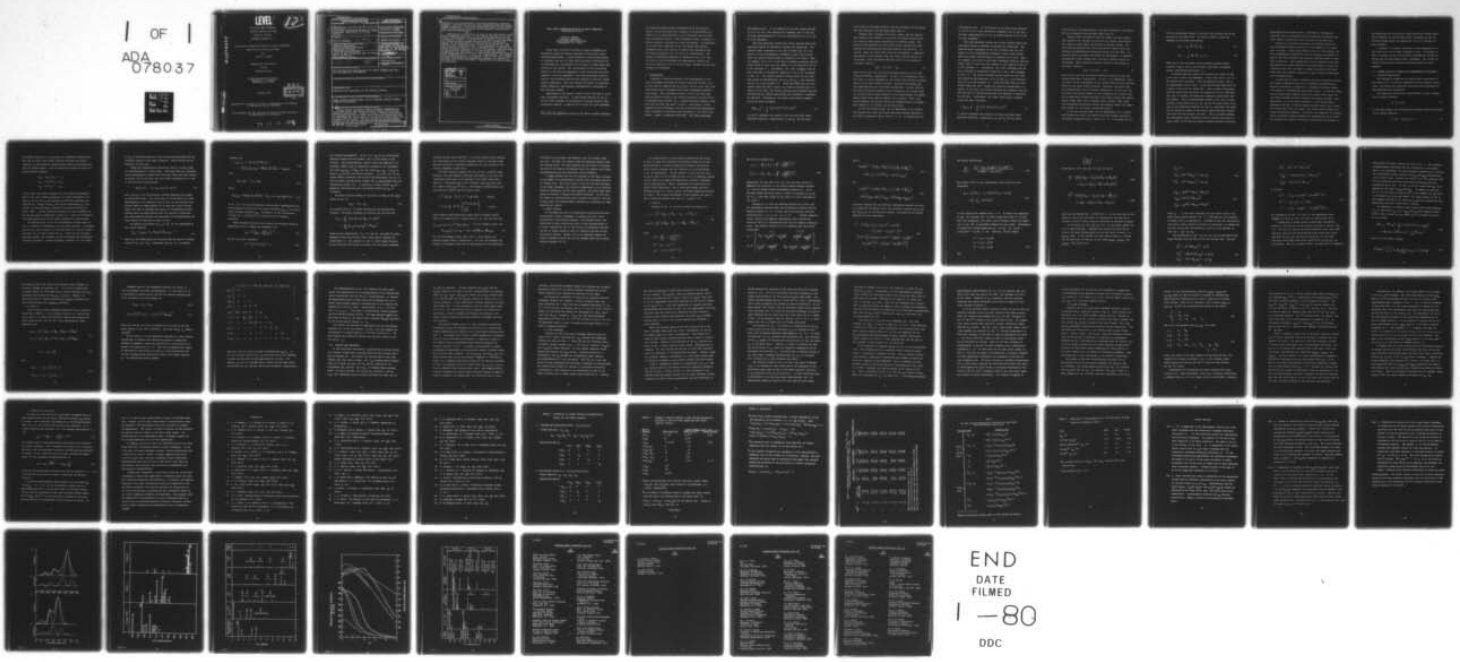

END
DATE FILMED
1-80
DDC

OFFICE OF NAVAL RESEARCH

Contract N00014-78-C-0496

Task No. 056-681

TECHNICAL REPORT NO. 1

Final State Correlation Effects in Auger Lineshapes; Application to Silicon Dioxide

by

David E. Ramaker

George Washington University
Department of Chemistry
Washington, DC 20052

Prepared for Publication

in the

Physical Review

November 1979

Unclassified

SECURITY CLASSIFICATION OF THIS PAGE (When Data Entered)

REPORT DOCUMENTATION PAGE		READ INSTRUCTIONS BEFORE COMPLETING FORM
1. REPORT NUMBER No. 1	2. GOVT ACCESSION NO.	3. RECIPIENT'S CATALOG NUMBER
4. TITLE (and Subtitle) Final State Correlation Effects in Auger Lineshapes; Application to Silicon Dioxide.		5. TYPE OF REPORT & PERIOD COVERED Technical Report,
		6. PERFORMING ORG. REPORT NUMBER
7. AUTHOR(s) David E. Ramaker		8. CONTRACT OR GRANT NUMBER(s) N00014-78-C-0496
9. PERFORMING ORGANIZATION NAME AND ADDRESS Chemistry Department George Washington University Washington, DC 20052		10. PROGRAM ELEMENT, PROJECT, TASK AREA & WORK UNIT NUMBERS Prog. Elem. No. 61153N Task Area No. RR 013-08-01 Work Unit No. NR 056-681
11. CONTROLLING OFFICE NAME AND ADDRESS Office of Naval Research, Dept. of Navy 800 N. Quincy St. Washington, DC 22217		12. REPORT DATE November 1979 13. NUMBER OF PAGES 58
14. MONITORING AGENCY NAME & ADDRESS(if different from Controlling Office) RR013 08		15. SECURITY CLASS. (of this report) Unclassified 15a. DECLASSIFICATION/DOWNGRADING SCHEDULE

16. DISTRIBUTION STATEMENT (of this Report)

This document has been approved for public release and sale; its distribution is unlimited.

17. DISTRIBUTION STATEMENT (of the abstract entered in Block 20, if different from Report)

18. SUPPLEMENTARY NOTES

Submitted for publication in the Physical Review.

19. KEY WORDS (Continue on reverse side if necessary and identify by block number)

Auger electron spectroscopy, silicon dioxide, surface oxides, electron correlation

20. ABSTRACT (Continue on reverse side if necessary and identify by block number)

Final state correlation effects in Auger lineshapes are considered within the cluster LCAO-MO-CI theory with a parameterized Hamiltonian. A model problem is solved analytically to elucidate the role of final state hole-hole correlation and to understand the localization of the holes on rather small subclusters of the system. The relationship of the correlation effects to the relative magnitudes of the one-center hole-hole

DD FORM 1 JAN 73 1473 EDITION OF 1 NOV 65 IS OBSOLETE
S/N 0102-014-6601

Unclassified

SECURITY CLASSIFICATION OF THIS PAGE (When Data Entered)

404 400

repulsion u and the bandwidth Γ has been previously reported; however, this previous work has been limited to metallic single element conductors. This work extends the theory to covalently bonded insulators (and possibly semiconductors) consisting of more than one element.

Application of the theory is made to the O KVV and Si $L_{23}VV$ Auger lineshapes from SiO_2. A high energy shoulder at 511 eV in the O KVV lineshape is interpreted as arising directly from correlation effects. A peak at 50 eV in the Si $L_{23}VV$ lineshape, its intensity significantly underestimated by the previous theory, is now accounted for; a peak at 70 eV previously suggested to be a shake satellite is now indicated also to arise from correlation effects. Both lineshapes reveal a density of states primarily localized on a Si_2O sub-cluster. The magnitude of the hole-hole repulsion on the sub-cluster and between neighboring Si_2O sub-clusters is empirically determined from the Auger lineshapes to be ∿ 11 and 4 eV, respectively. The oxygen 2p nonbonding bandwidth is estimated to be ∿ 6 eV, but in light of other theoretical and experimental results, our result is believed to be 1-2 eV too large. Reasons for our over-estimate are discussed.

FINAL STATE CORRELATION EFFECTS IN AUGER LINESHAPES; APPLICATION TO SiO_2*

David E. Ramaker
Chemistry Department
George Washington University
Washington, D.C. 20052

Final state correlation effects in Auger lineshapes are considered within the cluster LCAO-MO-CI theory with a parameterized Hamiltonian. A model problem is solved analytically to elucidate the role of final state hole-hole correlation and to understand the localization of the holes on rather small subclusters of the system. The relationship of the correlation effects to the relative magnitudes of the one-center hole-hole repulsion u and the bandwidth Γ has been previously reported; however, this previous work has been limited to metallic single element conductors. This work extends the theory to covalently bonded insulators (and possibly semiconductors) consisting of more than one element.

Application of the theory is made to the O KVV and Si $L_{23}VV$ Auger lineshapes from SiO_2. A high energy shoulder at 511 eV in the O KVV lineshape is interpreted as arising directly from correlation effects. A peak at 50 eV in the Si $L_{23}VV$ lineshape,

*This work was supported in part by the Office of Naval Research.

its intensity significantly underestimated by the previous theory, is now accounted for; a peak at 70 eV previously suggested to be a shake satellite is now indicated also to arise from correlation effects. Both lineshapes reveal a density of states primarily localized on a Si_2O sub-cluster. The magnitude of the hole-hole repulsion on the sub-cluster and between neighboring Si_2O sub-clusters is empirically determined from the Auger lineshapes to be ~11 and 4 eV, respectively. The oxygen 2p nonbonding bandwidth is estimated to be ~6 eV, but in light of other theoretical and experimental results, our result is believed to be 1-2 eV too large. Reasons for our overestimate are discussed.

I. INTRODUCTION

Recently we reported results of an investigation of the Auger lineshapes involving the valence electrons in SiO_2 (1,2). In this work we compared the Si $L_1L_{23}VV$, the Si $L_{23}VV$, and O KLL experimental Auger lineshapes with those lineshapes predicted from theory. The electronic structure of SiO_2 for this work was described in terms of one electron molecular orbitals (M.O.) on minimum-sized clusters (i.e., central atom plus nearest neighbors such as SiO_4^{4-} and Si_2O^{6+} in SiO_2). The results of this comparison were gratifying, with the calculated and experimental Auger lineshapes in generally good agreement in all three lineshapes. Figure 1 summarizes this data. The only significant

discrepancies are: (1) the absence of the high energy shoulder at 511 eV in the O KVV theoretical lineshape, and (2) the significant underestimation of the low energy peak at 50 eV in the Si $L_{23}VV$ lineshape.

That good agreement between the cluster LCAO-MO theory and experiment should be obtained is perhaps not surprising. The observed Auger lineshapes in the more covalent SiO_2 are very similar to the corresponding lineshapes in more ionic solids where the cluster LCAO-MO model is expected to be valid. Thus, for example, the S and P $L_{23}VV$ Auger lineshapes obtained from the highly ionic Li salts are very similar in all aspects to the Si $L_{23}VV$ lineshape (3). Furthermore, the O KVV lineshape from the more ionic MgO is essentially identical to the O KVV lineshape in SiO_2 (4). The valence electron energy levels for SiO_2 have been probed by photoemission, by Si K_β and $L_{2,3}$ x-ray emission, and by O K_α x-ray emission (5). These data have been well described within the SiO_4^{4-} cluster one electron LCAO-MO model (1); indeed, in our work, the orbital energies were obtained from the XPS data and the LCAO-MO populations were adjusted to reproduce the XES data. Furthermore, the atomic Auger matrix elements giving the Auger intensity

$$|M_{cab}|^2 = \sum_{kl} |\langle f_c\, kl\, |r_{12}^{-1}|\, f_a f_b\rangle|^2 \qquad (1)$$

(f_c and kl represent the original core hole and final state continuum functions, respectively; f_a and f_b, the two final

state holes in the Auger process) were not evaluated in our theory but were estimated from gas phase Auger data (2).

Despite these successes of the M.O. model, one can justifiably question the validity of utilizing the cluster one-electron M.O. model to study Auger transitions in covalent solids. The Auger process produces two final state holes, whereas the x-ray emission and photoemission processes produce just one hole. In general, these two final state holes see one another, a repulsive interaction U exist between them, and their relative motion is correlated. This interaction exhibits itself in the energy of the Auger electron,

$$E_{cvv'} = E_c - E_v - E_{v'} - U_{vv'} \qquad (2)$$

where the E's are the one-electron binding energies of core and valence electrons, respectively. In SiO_2, U is substantial, varying from 5 to 20 eV depending on the central atom and the localized nature of the final states involved. Hole-hole correlation may also substantially alter the Auger intensities. We note that the hole-hole correlation effects on the intensities of a single atom are in some sense already included in our model because the experimental atomic Auger matrix elements were utilized. Thus, only the interatomic correlation effects and banding effects are apparently absent in our earlier one-electron model.

In the one-electron model one can approximate U by a difference between two terms, the direct hole-hole Coulomb repulsion F and static relaxation term R, thus U = F - R. R accounts for the

discrepancies are: (1) the absence of the high energy shoulder at 511 eV in the O KVV theoretical lineshape, and (2) the significant underestimation of the low energy peak at 50 eV in the Si $L_{23}VV$ lineshape.

That good agreement between the cluster LCAO-MO theory and experiment should be obtained is perhaps not surprising. The observed Auger lineshapes in the more covalent SiO_2 are very similar to the corresponding lineshapes in more ionic solids where the cluster LCAO-MO model is expected to be valid. Thus, for example, the S and P $L_{23}VV$ Auger lineshapes obtained from the highly ionic Li salts are very similar in all aspects to the Si $L_{23}VV$ lineshape (3). Furthermore, the O KVV lineshape from the more ionic MgO is essentially identical to the O KVV lineshape in SiO_2 (4). The valence electron energy levels for SiO_2 have been probed by photoemission, by Si K_β and $L_{2,3}$ x-ray emission, and by O K_α x-ray emission (5). These data have been well described within the SiO_4^{4-} cluster one electron LCAO-MO model (1); indeed, in our work, the orbital energies were obtained from the XPS data and the LCAO-MO populations were adjusted to reproduce the XES data. Furthermore, the atomic Auger matrix elements giving the Auger intensity

$$|M_{cab}|^2 = \sum_{kl} |\langle f_c\, kl\, |r_{12}^{-1}|\, f_a f_b\rangle|^2 \qquad (1)$$

(f_c and kl represent the original core hole and final state continuum functions, respectively; f_a and f_b, the two final

state holes in the Auger process) were not evaluated in our theory but were estimated from gas phase Auger data (2).

Despite these successes of the M.O. model, one can justifiably question the validity of utilizing the cluster one-electron M.O. model to study Auger transitions in covalent solids. The Auger process produces two final state holes, whereas the x-ray emission and photoemission processes produce just one hole. In general, these two final state holes see one another, a repulsive interaction U exist between them, and their relative motion is correlated. This interaction exhibits itself in the energy of the Auger electron,

$$E_{cvv'} = E_c - E_v - E_{v'} - U_{vv'} \qquad (2)$$

where the E's are the one-electron binding energies of core and valence electrons, respectively. In SiO_2, U is substantial, varying from 5 to 20 eV depending on the central atom and the localized nature of the final states involved. Hole-hole correlation may also substantially alter the Auger intensities. We note that the hole-hole correlation effects on the intensities of a single atom are in some sense already included in our model because the experimental atomic Auger matrix elements were utilized. Thus, only the interatomic correlation effects and banding effects are apparently absent in our earlier one-electron model.

In the one-electron model one can approximate U by a difference between two terms, the direct hole-hole Coulomb repulsion F and static relaxation term R, thus U = F - R. R accounts for the

shift in the binding energy of one hole state orbital due to the presence of the other hole. In the M.O. model, F and R are expanded in the atomic equivalents

$$F_{vv'} = \sum_{ij} c^2_{vi}\, c^2_{v'j}\, F^\circ_{ij} + \cdots \qquad (3)$$

$$R_{vv'} = \sum_{ij} c^2_{vi}\, c^2_{v'j}\, r_i\, \delta_{ij} \qquad (4)$$

where the F° are the atomic Slater integrals between atomic orbitals i and j, and r_i is an atomic intra-shell relaxation energy, both defined previously (1).

A problem with the cluster one-electron M.O. model is that F and R are cluster size-dependent. Both F and R go to zero as the cluster size increases. Thus the question arises, what is the appropriate cluster size? In the one-electron band model for a solid, F and R are of course zero. This is merely consistent with the notion that the holes are completely free to roam about the solid or cluster, and hence are completely delocalized from one another. There is experimental evidence (6-8) that in some metallic solids, such as in Cu, Zn, and Ni, the final state holes, even in the conduction band, are not free to roam about the solid, but are forced to remain on the atom in which they were created (the atom with the initial core hole). This is evident because the experimental Auger intensity does not reflect the density of states (DOS) of the band but rather exhibits multiplet structure

consistent with an atomic model. Furthermore, the apparent magnitude of U is consistent with the hole-hole interaction one would expect if both holes were localized on the same atom.

Electron or hole-hole correlation in metallic solids has been considered within the context of the Hubbard (9) or Anderson (10) model. Within these models, Cini (11) and Sawatsky (12) have independently examined the role of electron correlation in metals, and have attributed the behavior indicated above to hole-hole correlation. More specifically, if the effective hole-hole interaction U is large compared to the band width Γ, energy conservation forces the two holes to remain localized on the atom where they were created, producing an Auger intensity consistent with the atomic model.

In this work we wish to consider hole-hole correlation within the cluster LCAO-MO-CI model with a parameterized Hamiltonian. Electron correlation in molecules is normally considered within the context of configuration interaction theory. It has the advantage of being easily applied within the cluster model where the two-center Coulomb repulsion integrals are easily included. More importantly, it can be easily applied to ionic and molecular insulators and more covalently bonded systems such as SiO_2, which may involve more than one element, and hence involve several different interaction energies. In Section 2 we summarize the general theory, providing working formulas for implementing the CI theory. To elucidate the effects of hole-hole correlation and attempt to

understand why the one-electron cluster molecular orbital model may be adequate for interpreting Auger lineshapes in some covalently bonded solids, we examine the role of CI mixing on a model problem.

In Section 3 we present numerical results appropriate for the O KVV and Si $L_{23}VV$ Auger lineshape in SiO_2. An attempt is made to account for the two described discrepancies between the theoretical and experimental Auger lineshapes. The effects of cluster size and the two-center Coulomb integrals are also examined.

II. CLUSTER LCAO-MO-CI THEORY WITH PARAMETERIZED HAMILTONIAN

1. General Formulations

The LCAO-MO-CI theory and its application to molecules is well known (13). We briefly summarize here the general formulations, also making the necessary definitions and indicating our approximations and limitations.

The molecular orbitals are constructed by a linear combination of atomic orbitals,

$$\varphi_\mu = \sum_i c_{\mu i} f_i \tag{5}$$

in the usual manner, the coefficients determined from the solution of the secular equation,

$$\Sigma_j \, (H_{ij} - \epsilon_\mu S_{ij}) c_{\mu j} = 0. \tag{6}$$

The atomic orbitals f_i at this point are completely unspecified; they may be Slater-type atomic orbitals, Hartree-Fock atomic orbitals, or even symmetry adapted atomic orbitals involving more than one atomic center. They are specified through the choice of orbital matrix elements,

$$H_{ii} = \langle f_i \mid \hat{h} \mid f_i \rangle = \alpha_i$$
$$H_{ij} = \langle f_i \mid \hat{h} \mid f_j \rangle = V_{ij}$$
$$S_{ij} = \langle f_i \mid f_j \rangle = \delta_{ij}. \qquad (7)$$

In this work, the matrix elements will be treated as parameters such as the tight binding parameters in a band calculation (14); that is, the α_i and V_{ij} are adjusted so that the resultant one-electron M.O. energy levels ϵ_μ and orbital populations $c_{\mu i}^2$ are similar to some previously determined one-electron density of states (DOS). We have reported previously our best estimates of the DOS and orbital populations in SiO_2 (1). They were determined from experimental data and ab-initio cluster M.O. calculations.

The decision here to set the off-diagonal overlaps equal to zero is a matter of convenience for this model problem. In general, they are not zero; however, it has been shown (15) that by including them, one in effect scales the V_{ij}. Since our V_{ij} are parameterized anyway, the ultimate effect of ignoring the off-diagonal overlaps is minimal. We have discussed elsewhere (16) the effect

of S_{ij} on the distribution of local versus bonding charge and the resultant effects on the Auger intensity. These effects are not important in this work.

Within the configuration interaction theory, we shall limit our considerations to filled bands. This means that all configurations describing the system after the Auger decay will have exactly two holes, and we can write the final state wavefunction as a sum of the two hole configurations,

$$\Psi_{vv'}(\bar{r}_1,\bar{r}_2) = \Sigma_{\alpha\beta} D_{vv',\alpha\beta} \varphi_\alpha(\bar{r}_1) \varphi_\beta(\bar{r}_2). \quad (8)$$

Here, the $\varphi_\mu(\bar{r})$ are the molecular orbitals spanning the cluster as constructed above. The restriction to filled bands is a good approximation in an insulator such as SiO_2, as the unfilled conduction bands are approximately 10 eV above the filled valence bands, and thus an insignificant amount of configuration mixing between these two bands should occur for realistic conditions. This approximation becomes less applicable for semiconductors and metals where the band gap is small or zero.

The mixing coefficients $D_{vv',\alpha\beta}$ in eq. (8) are determined by the secular equation

$$\sum_{\gamma\delta} (H_{\alpha\beta,\gamma\delta} - E_{vv'} S_{\alpha\beta,\gamma\delta}) D_{vv',\gamma\delta} = 0 \quad (9)$$

where the full Hamiltonian now includes both one and two electron terms $\hat{H} = \hat{h}_1 + \hat{h}_2 + \hat{U}_{12}$. Consistent with eq. (7), the matrix

elements are

$$H_{\alpha\beta,\gamma\delta} = \langle \phi_\alpha \phi_\beta | \hat{H} | \phi_\gamma \phi_\delta \rangle$$
$$= \langle \phi_\alpha | \hat{h}_1 | \phi_\gamma \rangle \delta_{\beta\delta} + \langle \phi_\beta | \hat{h}_2 | \phi_\delta \rangle \delta_{\alpha\gamma} + U_{\alpha\beta,\gamma\delta} \tag{10}$$

and

$$S_{\alpha\beta,\gamma\delta} = \delta_{\alpha\gamma}\,\delta_{\beta\delta} \tag{11}$$

where

$$U_{\alpha\beta,\gamma\delta} = \langle \phi_\alpha \phi_\beta | \hat{U}_{12} | \phi_\gamma \phi_\delta \rangle = \sum_{mn} c_{\alpha m}\, c_{\beta n} c_{\gamma m} c_{\delta n}\, u_{mn}. \tag{12}$$

In eq. (12), the zero differential overlap (ZDO) approximation has been employed to reduce the two center integrals $U_{\alpha\beta,\gamma\delta}$ to a sum of atomic Coulomb integrals u_{mn}. Throughout, we use the notation $\langle 12 | r_{12}^{-1} | 12 \rangle \equiv [1^2 | r_{12}^{-1} | 2^2]$ to indicate the two electron integrals.

Those integrals involving two centers are evaluated using an approximation due to Mataga and Nishimoto (17)

$$u_{mn} = e^2 \left[R_{mn} + \frac{2e^2}{(u_n + u_m)} \right]^{-1}, \tag{13}$$

and the one center integrals

$$u_n = [f_n^2 | r_{12}^{-1} | f_n^2] - r_n \tag{14}$$

are treated as parameters. In eq. (13), R_{mn} is the internuclear distance between the two centers, and e is the charge on the electron. This approximation, found in many semi-empirical M.O. programs, simply takes an appropriate average of two extremums; for large R_{nm}, $U_{mn} = e^2/R_{mn}$, for very small R_{mn}, $u_{mn} = (u_n+u_m)/2$, where u_n, u_m are the one center integrals. r_n in eq. (14) is the atomic static relaxation term as mentioned previously (see eq. 4); the one center Coulomb matrix element can be approximated from the tabulations of Mann (18). In practice, we have treated u_{mn} as a parameter observing hole-hole correlation effects as u_{mn} is increased.

The Auger electron energy is now given in terms of the eigenvalues of eq. (9)

$$E_{cvv'} = E_c - E_{vv'} \tag{15}$$

in contrast with eq. (2) which involved the one-electron M.O. energies. The Auger intensity now involves the two hole DOS

$$I_{cvv'} = \sum_{\ell} |\langle f_c\, k\ell\, |\, r_{12}^{-1}\, |\, \Psi_{vv'}(\vec{r}_1, \vec{r}_2)\rangle|^2$$

$$= \left|\sum_{\alpha\beta} D_{vv';\alpha\beta}\, c_{\alpha a}\, c_{\beta b}\right|^2 |M_{cab}|^2 \tag{16}$$

where we have inserted eqs. (1), (5), and (8), and made the usual assumption that only the one center Auger matrix elements are significant (1). The indices "a" and "b" label atomic orbitals on the atom with the initial core hole; thus the Auger lineshape

reflects the two hole local DOS. It is this feature which hastens the convergence of the cluster expansion result to the bulk limit and thus provides a reasonable probability for the success of the cluster expansion in this work.

The above analysis ignores the role of hole (electron) spin. Actually, the spin symmetry decreases the number of two hole configurations which have to be included in the final state wavefunction. Configurations of the "diagonal" type $\varphi_k\varphi_k$ only take the singlet form $\varphi_k\varphi_k\ 2^{-\frac{1}{2}}(\alpha\beta-\beta\alpha)$. Non-diagonal configurations can take both the singlet and the triplet forms

$$2^{-1/2}(\phi_k\phi_\ell+\phi_\ell\phi_k)\,2^{-1/2}(\alpha\beta-\beta\alpha) \qquad \text{singlet}$$

$$2^{-1/2}(\phi_k\phi_\ell-\phi_\ell\phi_k)\begin{Bmatrix}2^{-1/2}(\alpha\beta+\beta\alpha)\\ \alpha\alpha\\ \beta\beta\end{Bmatrix} \qquad \text{triplet}$$

Since singlet final states can couple only to singlet initial states (and similarly for triplet states), eq. (16) has the form

$$D_{vv',\alpha\alpha}\,c_{\alpha a}\,c_{\alpha b}\,2^{-1/2}(M_{cab}+M_{cba}) \qquad \text{for the diagonal terms, and}$$

$$D_{vv',\alpha\beta}\left[c_{\alpha a}c_{\beta b}\pm c_{\alpha b}c_{\beta a}\right](M_{cab}+M_{cba}) \qquad (17)$$

for the off-diagonal terms, where the +/- sign denotes the singlet/triplet states, respectively. For a=b, the diagonal and singlet off diagonal terms are the same except for the additional

$\sqrt{2}$ factor in the singlet off-diagonal term, the triplet terms are zero. For $a \neq b$, the triplet terms are generally smaller than the singlet terms. The spin symmetry has the effect of reducing the size of the secular determinant since the singlet and triplet configurations form non-interacting sub-determinants.

A common problem with the CI technique is the rapid increase in the number of configurations required with increasing molecule or cluster size. The local nature of the two hole DOS reflected in the Auger lineshape, the relative unimportance of the unfilled bands in insulators, and the spin symmetry, all points made above, assist us greatly in making the problem tractable. In this work the number of configurations never exceeded 50; however, this was in some cases the minimum number necessary for achieving our semi-quantitative results.

2. Model Problem.

To elucidate the role of configuration mixing and hole-hole correlation in Auger lineshapes, we examine here and solve analytically a four-orbital problem. As indicated above, the limitation to four orbitals and four or less configurations is a severe restriction, but it does retain the important features and yet is simple enough to offer an intuitive feeling for the correlation effects. Indeed, this is an important aspect the cluster LCAO-MO-CI model has over the Hubbard model which treats infinite systems (11,12).

The restriction to a four-orbital problem and the desire to have at least two identical sub-clusters limits us in this model problem to a linear system with triatomic sub-clusters B-A-B, where we assume that the orbitals on B are hybridized (e.g., sp hybridized). In this respect, B will play the role of the Si and A of the O atoms in SiO_2, as it is generally agreed (19,20) that Si is highly sp^3 hybridized, whereas O undergoes little hybridization. Table I summarizes two cases which are within these limitations, case a involving bonding and anti-bonding orbitals on A and B, case b involving nonbonding orbitals on atom A. The secular determinant is most general for case a; case b being the special case when $\alpha_O = \alpha_H$ and $V = \Gamma$.

2. (Case a)

Solution of eq. (6) for case a gives the four M.O.'s

$$|i/ii\rangle = N_{\pm}^{1/2}\left(\phi_{A1} + a^{\pm}\phi_{H1} \pm \phi_{A2} \pm a^{\pm}\phi_{H2}\right)$$

$$|iii/iv\rangle = N_{\pm}^{1/2}\left(a^{\pm}\phi_{A1} - \phi_{H2} \pm a^{\pm}\phi_{A2} \mp \phi_{H2}\right) \tag{18}$$

where

$$a^{\pm} = \frac{A^{\pm}}{2V} + \sqrt{\left(\frac{A^{\pm}}{2V}\right)^2 + 1}$$

$$A^{\pm} = \alpha_H - \alpha_A \pm \Gamma$$

$$N^{\pm} = 1/\left[2\left(1+(a^{\pm})^2\right)\right] \tag{19}$$

and the M.O. energies are

$$\varepsilon_{i/ii} = \varepsilon_b^{\pm} = \alpha_A + \frac{A^{\pm}}{2} + \sqrt{\left(\frac{A^{\pm}}{2}\right)^2 + V^2}$$

$$\varepsilon_{iii/iv} = \varepsilon_a^{\pm} = \alpha_A + \frac{A^{\pm}}{2} - \sqrt{\left(\frac{A^{\pm}}{2}\right)^2 + V^2} \quad . \tag{20}$$

Appropriate for the case, $\Gamma << V$, eq. (20) has been written to emphasize the existence of two closely spaced bonding orbitals $\varepsilon_b^{\pm}$, and two closely spaced antibonding orbitals $\varepsilon_a^{\pm}$. In an extended system one would obtain a "band" of energies at ε_b and one at ε_a, with band widths of the order of Γ and a band gap of the order V.

Assuming in "a" that the bonding orbitals are filled, and the antibonding orbitals empty and sufficiently removed from the bonding orbitals ($V > U$), we have just three possible two-hole configurations: $|i,i\rangle$, $|iii,iii\rangle$, and $|i,ii\rangle$. Further simplification results from symmetry requirements which exclude any mixing of the $|i,ii\rangle$ configuration with the two diagonal configurations. The problem reduces to a 2 x 2 problem with the secular determinant

$$\begin{array}{c} \\ \langle i,i| \\ \langle iii,iii| \end{array} \begin{array}{c} \begin{array}{cc} |i,i\rangle & |iii,ii\rangle \end{array} \\ \begin{bmatrix} 2\varepsilon_b^{+} + \frac{U_1(AH)^{++}}{2} + \frac{U_{12}(AH)^{++}}{2} & \frac{U_1(AH)^{+-}}{2} - \frac{U_{12}(AH)^{+-}}{2} \\ \frac{U_1(AH)^{+-}}{2} - \frac{U_{12}(AH)^{+-}}{2} & 2\varepsilon_b^{-} + \frac{U_1(AH)^{--}}{2} + \frac{U_{12}(AH)^{--}}{2} \end{bmatrix} \end{array} \tag{21}$$

where

$$U_1(AH)^{\pm\pm} = \left[\left(\phi_A + a^{\pm}\phi_H\right)_1^2 \left| r_{12}^{-1} \right| \left(\phi_A + a^{\pm}\phi_H\right)_1^2\right]$$
$$= 4N_{\pm}^2 \left[u_A + (a^{\pm}a^{\pm})^2 u_H + 2a^{\pm}a^{\pm} u_{A,H_1}\right] \tag{22}$$

and

$$U_{12}(AH)^{\pm\pm} = \left[\left(\phi_A + a^{\pm}\phi_H\right)_1^2 \left| r_{12}^{-1} \right| \left(\phi_A + a^{\pm}\phi_H\right)_2^2\right]$$
$$= 4N_{\pm}^2 \left[u_{A_1A_2} + (a^{\pm}a^{\pm})^2 u_{H_1H_2} + a^{\pm}a^{\pm}\left(u_{A_1H_1} + u_{A_2H_1}\right)\right] \tag{23}$$

represent respectively the effective interaction between two holes on a single B-A-B cluster and on two different clusters (B_1-A_1-B_2) and (B_2-A_2-B_3) in the four atom system. Solutions of the secular equation give the eigenvalues

$$E^{\pm} = \left[4\left(\varepsilon_b^{+} + \varepsilon_b^{-}\right) + U_1(AH)^{++} + U_1(AH)^{--} + U_{12}(AH)^{++} + U_{12}(AH)^{--}\right]/4$$
$$\pm \tfrac{1}{2}\,\mathrm{SQRT}\left\{\left[4\left(\varepsilon_b^{+} - \varepsilon_b^{-}\right) + U_1(AH)^{++} - U_1(AH)^{--} + U_{12}(AH)^{++} - U_{12}(AH)^{--}\right]^2/4 + \left[U_1(AH)^{++} - U_{12}(AH)^{+-}\right]^2\right\} \tag{24}$$

and mixing coefficients

$$\frac{D_{ij}}{D_{ii,ii}} = \frac{2E^{\pm} - 4\epsilon_b^{+} - (U_1(AH)^{++} + U_{12}(AH)^{++})}{U_1(AH)^{+-} - U_{12}(AH)^{+-}} \quad . \tag{25}$$

The energy of the |i,ii> configuration can be given by the expression

$$\begin{aligned} E_o &= \langle 2^{-\frac{1}{2}}(i,ii + ii,i)|\hat{H}|2^{-\frac{1}{2}}(i,ii + ii,i)\rangle \\ &= \epsilon_b^{+} + \epsilon_b^{-} + U_1(AH)^{+-} . \end{aligned} \tag{26}$$

It has already been assumed that U << V. To reduce the complexity of eqs. (24) through (26), we shall assume here that $\Gamma << U_1(AH)$. With this assumption, the first term in brackets inside the square root in eq. (24) is negligible compared to the second. Furthermore, we define the average quantities $\epsilon_b = 1/2(\epsilon_b^{+} + \epsilon_b^{-})$, $U_1(AB) = 1/2(U_1(AB)^{++} + U_1(AB)^{--})$, etc. Then eqs. (24-26) become

$$\begin{aligned} E^{-} &= 2\,\epsilon_b + U_{12}(AB) \\ E^{\circ} &= 2\,\epsilon_b + U_1(AB) \\ E^{+} &= 2\,\epsilon_b + U_1(AB) \end{aligned} \tag{27}$$

and

$$\left(\frac{D_{11}}{D_{22}}\right)^{\pm} = \pm 1. \tag{28}$$

Inserting eq. (28) into eqs. (8) and (18) gives

$$\Psi^{-} = \sqrt{2}N\left[(\phi_{A1}+a\phi_{H1})(1)(\phi_{A2}+a\phi_{H2})(2) + (\phi_{A2}+a\phi_{H2})(1)(\phi_{A1}+a\phi_{H1})(2)\right] \tag{29a}$$

$$\Psi^{\circ}_{+} = \sqrt{2}N\left[(\phi_{A1}+a\phi_{H1})(1)(\phi_{A1}+a\phi_{H1})(2) \mp (\phi_{A2}+a\phi_{H2})(1)(\phi_{A2}+a\phi_{H2})(2)\right] \tag{29b}$$

where we have defined $Na = 1/2(N^{+}a^{+}+N^{-}a^{-})$. It is clear that in the states Ψ^{+} and Ψ° the two holes are localized on the same B-A-B cluster; in the Ψ^{-} state, they are localized on different clusters.

If we insert eq. (29) into eq. (16), we can obtain either the A or B Auger intensity. Assuming the initial core hole was on atom A_1, the Auger process picks out the DOS local on atom A_1, or $\varphi_{A1}\varphi_{A1}$ terms. If the initial core hole was on atom B_2, it picks out the DOS local on atom B_2, or the terms $\varphi_{H1}\varphi_{H1}$, $\varphi_{H1}\varphi_{H2}$, and $\varphi_{H2}\varphi_{H2}$. The results are

$$I^{-}_{A1} = 0$$

$$I^{o}_{A1} = 2N^2 |M_{cAA}|^2 = \tfrac{1}{2} I_A \qquad (30)$$

$$I^{+}_{A1} = 2N^2 |M_{cAA}|^2 = \tfrac{1}{2} I_A$$

$$I^{-}_{B2} = \tfrac{1}{2} N^2 a^4 |M_{css} - M_{cpp}|^2$$

$$I^{o}_{B2} = 2N^2 a^4 |M_{csp}|^2 \qquad (31)$$

$$I^{+}_{B2} = \tfrac{1}{2} N^2 a^4 |M_{css} + M_{cpp}|^2$$

where I_A is the total intensity for the "band" and M is the atomic Auger matrix element (eq. (1)) involving the core orbitals on atoms A and B as appropriate. Although we have not specifically introduced s and p orbitals on atom B to this point, we assume here for convenience that the orbitals h_1 and h_2 are sp hybrids, so that $s(p) = \frac{1}{\sqrt{2}} (h_1 \pm h_2)$.

The intensities in eqs. (30) and (31) can be contrasted with those obtained from the fold of the one electron DOS. They are

$$I^{ii,ii}_{A1} = N_-^2 |M_{cAA}|^2 \approx \tfrac{1}{4} I_A$$

$$I^{i,ii}_{A1} = 2N_+N_- |M_{cAA}|^2 \approx \tfrac{1}{2} I_A \qquad (32)$$

$$I^{ii}_{A1} = N_+^2 |M_{cAA}|^2 \approx \tfrac{1}{4} I_A$$

$$I_{B2}^{ii,ii} = N_+^2 (a^-)^4 |M_{cpp}|^2$$

$$I_{B2}^{i,ii} = 2N_-N_+ (a^+a^-)^2 |M_{csp}|^2 \qquad (33)$$

$$I_{B2}^{i,i} = N_-^2 (a^+)^4 |M_{css}|^2$$

at energies

$$E^{ii,ii} = 2\varepsilon_b^- + (U_1(AH)^{--} + U_{12}(AH)^{--})/2$$

$$E^{i,ii} = \varepsilon_b^+ + \varepsilon_b^- + U_1^{+-}(AH) \qquad (34)$$

$$E^{i,i} = 2\varepsilon_b^+ + (U_1(AH)^{++} + U_{12}(AH)^{++})/2 .$$

The intensities in eqs. (30) and (31) are appropriate when $\Gamma \ll U_1(AB) \ll V$; those in eqs. (32) and (33) when $U_1(AB) \ll \Gamma \ll V$.

A comparison of these results reveals some interesting features. For the case of the initial core hole on atom A, eqs. (27), (30) and (32) reveal an overall shifting of the same total intensity from the term involving non-local final state holes (one hole on B_1-A_1-B_2; the other on B_2-A_2-B_3) to the terms involving local final state holes (both holes on B_2-A_1-B_2) as U increases. This is a general result, one which will be examined

numerically for larger clusters in SiO_2 in Sec. 3. The situation is significantly different when the initial hole is on atom B. First, as U_1 increases, the total intensity changes due to increasing interference effects between the M_{css} and M_{cpp} contributions in the large U case. Second, even when $U \gg \Gamma$, the intensity from the term involving non-local final states holes I^-_{B2} does not necessarily go to zero. In fact, it may be larger than I^+_{B2}; this depends on the signs of M_{css} and M_{cpp}. In summary, we can say for $U \gg \Gamma$, the Auger process on the A_1 atom samples the DOS local to the smaller B_1-A_1-B_2 sub-cluster; the Auger process on the B_2 atom samples the DOS on the larger B_1-A_1-B_2-A_2-B_3 cluster but with significant hole-hole "correlation" effects.

An examination of several cases reveals that quite generally $I^+_{B_2}$ is less than $I^-_{B_2}$; i.e., M_{cpp} and M_{css} have opposite signs. For the case at hand, the sp_z hybrid and a 1s initial core hole on B_2, we have

$$\begin{aligned}(M_{css} \pm M_{cpp})^2 &= \sum_{\ell} \langle 1s\, k\ell \,|\, r_{12}^{-1} \,|\, (ss + p_z p_z)\rangle^2 \\ &= \left(R^0(ssss) \pm \tfrac{1}{2} R^0(sspp)\right)^2 \pm \tfrac{4}{45} R^2(sd_{pp})^2\end{aligned} \tag{35}$$

where R is the radial integral

$$R^k(s\ell\ell'\ell') = \int_0^\infty \int_0^\infty R_{1s} R_{k\ell} \left|\frac{r_<^k}{r_>^{k+1}}\right| R_{n\ell' n\ell'} r_1^2 r_2^2 \, dr_1 \, dr_2 . \tag{36}$$

For atoms in the first rows of the periodic table, $\overset{o}{R}(ssss)$ is positive, $\overset{o}{R}(sspp)$ is negative (21). For the K-LL transitions in atoms, Asaad (22) has found that CI effects decrease the KL_1L_1 intensity and increase the $KL_{23}L_{23}$ intensity. McGuire (23) determined that CI effects decrease the $L_{23}M_1M_1$ intensity in Cu and Zn and increase the $L_{23}M_{23}M_{23}$ intensity.

2.2 (Case b)

Case b involves four nonbonding orbitals on four A atoms as indicated in Table I. It is a special case of "a", namely when $\epsilon_O=\epsilon_H$, and V = Γ; hence the molecular orbitals and energies are still given by eqs. (18) to (20). More specifically, these equations give

$$|i/ii\rangle = N_{\pm}^{1/2}\left(\phi_{A1} + a^{\pm}\phi_{A2} \pm \phi_{A3} \pm a^{\pm}\phi_{A4}\right)$$
$$|iii/iv\rangle = N_{\pm}^{1/2}\left(\phi_{A1} - a^{\pm}\phi_{A2} \pm \phi_{A3} \mp a^{\pm}\phi_{A4}\right) \qquad (37)$$

$$a^{\pm} = \pm\frac{1}{2} + \sqrt{\frac{5}{4}} \qquad (38)$$

and

$$\epsilon_{i/ii} = \alpha_A + \frac{\Gamma}{2}\left(\sqrt{5} \pm 1\right)$$
$$\epsilon_{iii/iv} = \alpha_A + \frac{\Gamma}{2}\left(-\sqrt{5} \pm 1\right). \qquad (39)$$

Assuming that all the nonbonding orbitals are filled, we have ten possible two-hole configurations. In the event $U \ll \Gamma$, a negligible CI mixing occurs, and the two electron energies and Auger intensities are given simply as

$$E_{\alpha\beta} = \varepsilon_\alpha + \varepsilon_\beta \tag{40}$$

$$I_{\alpha\beta} : \left[(a^+)^2, (a^-)^2, \text{ or } (a^+a^-) \right] \left| M_{cAA} \right|^2 \tag{41}$$

where the initial core hole is assumed to be on atom A_2 and the proper choice in eq. (41) is obvious. The total sum $\sum_{\alpha\beta} I_{\alpha\beta}$ equals $\left| M_{cAA} \right|^2$.

In the event $U \approx \Gamma$, the analytical solution of a 10x10 secular determinant is formable even though the problem is simplified somewhat by symmetry. Much more instructive at this point is to examine the problem when $U \gg \Gamma$. This can be examined more simply by omitting the construction of the M.O.'s and constructing the two-hole configurations directly in terms of the atomic orbitals φ_A. The Hamiltonian matrix becomes

$$
\begin{array}{c|cccccccccc}
 & |11\rangle & |22\rangle & |33\rangle & |44\rangle & |12\rangle & |23\rangle & |34\rangle & |13\rangle & |24\rangle & |14\rangle \\
\hline
\langle 11| & u_1 & & & & & & & & & \\
\langle 22| & 0 & u_1 & & & & & & & & \\
\langle 33| & 0 & 0 & u_1 & & & & & & & \\
\langle 44| & 0 & 0 & 0 & u_1 & & & & & & \\
\langle 12| & \sqrt{2}\Gamma & \sqrt{2}\Gamma & 0 & 0 & u_{12} & & & & & \\
\langle 23| & 0 & \sqrt{2}\Gamma & \sqrt{2}\Gamma & 0 & 0 & u_{12} & & & & \\
\langle 34| & 0 & 0 & \sqrt{2}\Gamma & \sqrt{2}\Gamma & 0 & 0 & u_{12} & & & \\
\langle 13| & 0 & 0 & 0 & 0 & \Gamma & \Gamma & 0 & u_{13} & & \\
\langle 24| & 0 & 0 & 0 & 0 & 0 & \Gamma & \Gamma & 0 & u_{13} & \\
\langle 14| & 0 & 0 & 0 & 0 & 0 & 0 & 0 & \Gamma & \Gamma & u_{14}
\end{array}
\tag{42}
$$

where the $|ij\rangle$ now refer to atomic configurations $\varphi_{Ai}\varphi_{Aj}$. In eq. (42) we have omitted the 2 α_A term from each of the diagonal elements and utilized the ZDO approximation as usual. The symbols u_{ij} refer to Coulomb matrix elements on the same center and between the 1st, 2nd and 3rd nearest neighbors, respectively.

The diagonalization of eq. (42) produces the same eigenvalues and eigenvectors as the diagonalization of the Hamiltonian matrix constructed from the ten M.O. configurations. In general, the Hamiltonian matrix is more difficult to diagonalize in the atomic basis because symmetry considerations do not simplify the problem as in the M.O. basis. Nevertheless, if $u_i >> \Gamma$ and thus also $(u_i - u_{ij})_{i \neq j} >> \Gamma$, this matrix is essentially already diagonal and the solution becomes trivial. The Auger process samples the DOS local on atom A_2; the entire Auger intensity $|M_{cAA}|^2$ coalesces to one narrow peak at energy $2\alpha_a + u_1$.

The case"b" as described is appropriate for the non-bonding orbitals on O in the SiO_2 system. In Sec. 3 we will examine the coalescence to a single peak as u_i increases relative to Γ, and also examine the effects of cluster size and the effects of the two center u_{ij}.

III. RESULTS AND DISCUSSION

We have performed various M.O. calculations on several different clusters, always with a minimal basis set and at times with a partial minimal set. The valence one electron DOS in SiO_2 fall roughly into three major groups: the "O_{2s}" bonding states grouped about 20 eV below the edge (the $4a_1$ and $3t_2$ orbitals of the tetrahedral SiO_4 cluster), the "O_{2p}" (b) bonding states grouped about 6 eV below the edge (the $5a_1$ and $4t_2$ orbitals), and the "O_{2p}" (nb) nonbonding states located just below the edge (the 1e,

$5t_2$ and $1t_1$ orbitals). We have examined the $O_{2p}(b)$ and the $O_{2p}(nb)$ states on the Si_4O_3 and Si_8O_7 clusters with O as central atom, the O_{2s}, $O_{2p}(b)$ and $O_{2p}(nb)$ states on a Si_5O_4 cluster with Si as central atom, and the $O_{2p}(nb)$ density of states on O_3, O_7, and O_{16} clusters. A beta crystobalite crystal structure (Si-O-Si angle equal 180°) is used throughout with Si-O bond length equal 1.5 Å (24). The initial core hole is placed in a central Si_2O sub-cluster, nearest neighbor sub-clusters are placed in the proper crystal structure building outwardly to assemble the complete cluster.

The matrix elements in eq. (6) were treated as parameters, determined so that the resultant one electron M.O. energies and orbital populations are similar to our previously determined SiO_2 DOS (1). An optimal set of matrix element parameters, determined from the above-indicated calculations, is reported in Table II and compared with corresponding tight binding parameters as recently reported (14,25). In general, the agreement is quite satisfactory considering our calculations involve a minimal basis set on rather small clusters. The $V(O_{2s},O_{2s})$ and $V(O_{2p},O_{2p})$ elements include both direct and indirect "hopping" or interaction terms, i.e., hopping terms which involve the Si atom are included. In fact, the presence of the Si atoms in the O_{16} $O_{2p}(nb)$ calculation is exhibited only through these terms. Only hopping matrix elements involving two oxygen atoms connected through a common Si atom are assumed to be significant, all others are set to zero.

Likewise, only nearest neighbor bonded Si-O elements are included. Appropriate values for the matrix elements involving the Si sp^3 hybrid orbital h_i are obtained as indicated in the table.

The values of u tabulated in Table II are obtained from the integrals of Mann (18); however, a static relation term r has been subtracted off. These have been estimated previously (1) to be 6 eV for O2s and 2p orbitals, and 2(1) eV for Si 3s(3p) orbitals. Huang (15) has given the formula for obtaining the $u(Si_h)$ result from the $u(Si_{3s/p})$ elements. $u(O_{2p})$ has also been determined empirically by Oleari et. al. (26) who obtained a value of 14.5 eV. The empirical result is said to include correlation effects (i.e., static relaxation effects).

1. O KLL Lineshape

Results for the O KLL Auger lineshape obtained from the linear Si_4O_3 cluster involving the "O_{2p}" bonding and nonbonding orbitals are given in Fig. 2. These results were obtained from a 12-orbital system; namely 3 $Si_H = 1/\sqrt{2}\ (h_1-h_2)$ orbitals, 3 $O_{2p}(b)$, and 6 $O_{2p}(nb)$ atomic orbitals. In this system, symmetry allows mixing only between the O_{2pz} and Si_H orbitals giving M.O.'s belonging to the O_{2p} bonding and antibonding groups; however, the antibonding M.O.'s are unoccupied. Thus the b-b, b-nb, and nb-nb two-hole configurations are mixed in separate CI calculations. The results show clearly the effects of increasing correlation (increasing u), most notably in the coalescence of most of the Auger intensity into a rather narrow band around 502 eV. Clearly,

this band corresponds to both holes localized on to the same Si-O-Si cluster. The O_{2p}(nb) lines are shifted down by ~15 eV as they are localized on a single O atom; the O_{2p}(b) lines just 11 eV (the approximate hole-hole repulsion on the Si-O-Si cluster in the O_{2p}(b) M.O.). Note the appearance of residual non-local contributions shifted down by just 4 eV (the approximate hole-hole repulsion when the holes are on different Si-O-Si clusters). Ignoring these residual contributions, the Auger O_{2p} lineshape narrows from ~9 eV to ~2 eV, giving essentially an atomic O Auger spectrum.

Since the greatest share of the 502 eV peak of the O KLL Auger lineshape comes from the (nb,nb) transitions, we can for the moment ignore all other contributions. This allows for a study of much larger clusters and hence also a study of cluster size effects. Results of calculations on the O_{16} clusters are given in Fig. 3, where just the Auger (nb,nb) contributions are examined. The one electron DOS and the two hole DOS resulting from a CI involving 37 configurations are shown. Similar trends are revealed, namely a coalescence to a local peak shifted down in energy by an amount u_1 and several residual non-local peaks.

Figure 5 summarizes results of calculations on O_3, O_7, and O_{16} clusters when all two-center hole-hole repulsion integrals are set to zero. Plotted in Fig. 4 is the intensity in the residual non-local peaks relative to the total intensity (always normalized to 100 in these calculations) and the difference in

energy between the centriods of the local and non-local contributions vs. u/Γ. u/Γ is the one-center hole-hole repulsion on the oxygen atom divided by the one electron $O_{2p}(nb)$ band width. The results plotted depend only on u/Γ and not on u and Γ, individually, and no other parameters are present in these calculations. As one might expect, the results from the different cluster sizes converge with increasing u/Γ; for large u/Γ the Auger lineshape is increasingly dominated by the local peak where both holes are on a single O atom. In the physical range of interest, $u/\Gamma \approx 2$ to 4, it would appear that the O_7 cluster size is already sufficient.

Also plotted in Fig. 4 is result of a calculation on the O_{16} cluster when the two-center integrals u_{ij} are included as estimated from the Mataga-Mishimoto approximation, eq. (13). In these calculations, the u_{ij} increase with increasing u/Γ. The inclusion of the u_{ij} appears to decrease the effective size of the one-center u_i, as one might expect. However, it should be pointed out that the full effects of u_{ij} cannot be completely compensated for by decreasing the effective u_i. The shift down in absolute energy of the total Auger lineshape increases when the u_{ij} are included, but a decrease in u_i would decrease this shift.

The difference peak at 511 eV in the O KLL Auger lineshape (Fig. 1) is estimated to have about 20% of the intensity of the theoretical Auger peak at 504 eV (the shake satellite intensity is not included in the 504 eV peak here). If this difference peak is attributed to the non-local Auger contributions, the 7 eV experimental separation between the local and non-local peaks

provides an estimate of 2.5 for u/Γ (from Fig. 4, using the O_{16} nonzero u_{ij} plot). Furthermore, the 17% experimental intensity ratio between the difference peak at 511 eV and the total (504 eV peak plus 511 eV peak) indicates a u/Γ value of 2.5 (also from Fig. 4, non-zero u_{ij} plot). That the two estimates are in agreement is most gratifying and supports rather strongly the assumption that the 511 eV shoulder is indeed due to the non-local contributions. Note that the O_{16} results obtained for zero u_{ij} would give conflicting values for u/Γ.

The value of 2.5 for u/Γ is a reasonable one. The best estimate of $u(O_{2p})$, as given in Table II, is 15 eV. This indicates a value of 6 eV for Γ. Band calculations (14,19,20,25,27,28) have given results varying from 1 to 5 eV for the bandwidth of the O_{2p} nonbonding band with perhaps the most reliable theoretical result around 5 eV (20,27). X-ray emission data and UPS data in SiO_2 suggest a value around 4 eV (27,29,30,31).

We can suggest two possible causes for our 1-2 eV overestimate of Γ. The determination of a bandwidth from a relatively small cluster calculation is nebulous at best. The O_{16} cluster calculations provide a spectrum of eigenvalues, the breadth of which provides our estimate of the bandwidth. This is probably the best procedure since in band calculations, Γ represents the full width of the DOS. Secondly, our results depend on the values of the u_{ij}. This is indicated in Fig. 5 for the two O_{16} cluster calculation, one including the u_{ij}, the other not. If the Mataga-Nishimoto

approximation underestimates the u_{ij} (we will present some evidence later that this may be the case), our estimate of Γ will be too large. Evidently as u_{ij} increases, both the relative intensity and energy difference curves move to higher u/Γ and hence indicate a smaller Γ.

It is of interest from an intuitive point of view to note the relative location of the two holes formed in the Auger process. Table III contains the probabilities P_{ij} for hole occupancy on the i^{th} and j^{th} O atoms in the O_{2p}(nb) band of SiO_2. For simplicity, these results come from an O_7 cluster calculation rather than the O_{16} cluster. The two "local" Auger peaks, peaks 4 and 5 (peak numbers are indicated in Fig. 3), clearly correspond to a high hole occupancy on the same O atoms as anticipated for large u. The three "non-local" peaks in order of decreasing energy can be described as follows: peak (3) the hole occupancy is predominantly on 2nd and 3rd near neighbors with a significant probability (~.11) for both holes on the same center; peaks (2) and (1), the hole occupancy is predominantly on nearest neighbors but with significant probability for occupancy on 2nd and 3rd near neighbors also. The Auger intensity is directly proportional to P_{11} (both holes occupying the atom with the initial core hole). It would appear the Auger energy is primarily determined by the total of the one center occupancy terms as the "non-local" peaks are ordered in energy accordingly. The relative occupancy of

nearest neighbors and 2nd and 3rd near neighbors is unimportant in determining energy apparently because the 1/R behavior reduces u_{12} already to ~4 eV (when u_1 is 15 eV), and the higher terms (e.g., u_{13}, u_{25}, etc.) are only slightly smaller.

2. Si $L_{23}VV$ Lineshape

Results for the Si $L_{23}VV$ Auger lineshape obtained from the tetrahedral Si_5O_4 cluster is given in Fig. 6. These results were obtained from a 16 orbital system; namely four Si_h orbitals on the central Si, one Si_h orbital on each of the edge Si atoms, and an O 2s and $2p_z$ orbital on each of the four O atoms. The O $2p_x$ and $2p_y$ nonbonding orbitals were ignored in this calculation. The resultant one electron M.O.'s are named in the T_d point group $4a_1(3s)$, $3t_2(3p)$, $5a_1(3s)$, and $4t_2(3p)$, where the dominant contribution of the Si atom in each M.O. is indicated in parentheses. Although the M.O. calculations are performed with sp^3 hybrids (h_i) on the Si atoms, solution of the secular equation automatically provides for the proper linear combination of these hybrids to give back either an s or p orbital as dictated by symmetry. Upon performing the CI with increasing u_i, the orbitals rehybridize.

The number of two-hole configurations necessary for an appropriate hole-hole correlation treatment can again be kept to a minimum. The energy spacing between the $4a_1$, $3t_2$ orbitals (the O_{2s} band) and the $5a_1$, $4t_2$ orbitals (the $O_{2p}(b)$ band) is large compared to the effective hole-hole repulsion in the Si_5O_4

cluster, so the configurations from the O_{2s}-O_{2s}, O_{2s}-O_{2p} and O_{2p}-O_{2p} bands can again be mixed in separate CI calculations. Group theoretic arguments can be used to simplify the problem still further. Thus in the "diagonal" cases (either O_{2s}-O_{2s} or O_{2p}-O_{2p}), we have the configurations leading to the terms:

$$\begin{aligned} a_1^2 &- {}^1A_1 \\ a_1 t_2 &- {}^1T_2, {}^3T_2 \\ t_2^2 &- {}^1A_1, {}^3T_1, {}^1E, {}^1T_2 \end{aligned} \tag{43}$$

and in the non-diagonal case O_{2s}-O_{2p}, the terms:

$$\begin{aligned} a_1 a_1' &- {}^1A_1, {}^3A_1 \\ a_1 t_2' &- {}^1T_2, {}^3T_2 \\ a_1' t_2 &- {}^1T_2, {}^3T_2 \\ t_2 t_2' &- {}^1A_1, {}^3A_1, {}^1T_2, {}^3T_2, {}^1E, {}^3E, \\ &\qquad {}^1T_1, {}^3T_1 . \end{aligned} \tag{44}$$

Since only terms of the same symmetry and multiplicity mix, the complete CI is easily tractable (e.g., in the diagonal cases, mixing occurs only between the two ^1A terms and only between the two $^1T_2$ terms).

Expressions for determining the Auger intensity are given in Table III. These expressions involve the CI mixing coefficients D obtained from eq. (9), the atomic orbital coefficients c obtained

from solution of eq. (6), and the atomic Auger matrix elements in L-S coupling $M_{c\ell\ell'}(^{2S+1}L)$. Expressions for evaluating $M_{c\ell\ell'}(^{2S+1}L)$ have been reported by McGuire (23) and others (22,32,33). The $M_{cpp}(^3S)$, $M_{cpp}(^3D)$, $M_{cpp}(^1P)$, and $M_{css}(^3S)$ matrix elements are zero in this work, as shown in eq. (17) and sec. II.1. The five ^1D terms in spherical symmetry split into the ^1E and $^1T_2$ terms in tetrahedral symmetry. The ^1D intensity splits up equally, one-fifth into each of the terms regardless of symmetry (34). As determined by McGuire, $M_{css}(^1S)$ and $M_{cpp}(^1S)$ are of different sign so that the $a_1^2 + t_2^2$ state has a smaller intensity than the $a_1^2 - t_2^2$ state.

Figure 5 compares results with no hole-hole repulsion effects, with hole-hole repulsion effects but without CI mixing, and with complete CI mixing. The turn on of hole-hole repulsion without CI mixing causes additional lines from multiplet splitting. The turn on of CI mixing then coalesce these terms into "local" and "non-local" contributions for each band (O_{2s}-O_{2s}, O_{2s}-O_{2p}, and O_{2p}-O_{2p}). In this instance, the local contributions correspond to both holes localized on an Si_2O sub-cluster with $U_{eff} \approx 11$ eV, and the non-local contributions to the holes localized on different Si_2O sub-clusters with $U_{eff} \approx 4$ eV. Because the initial core hole was on the central Si atom with a local Si population in all four Si_2O sub-clusters, the Auger intensity now does not coalesce into just the local peak as in the O KLL case, but a major part of the Auger intensity remains in the non-local contributions.

Nevertheless, the effects of CI mixing appear to be evident in the Si $L_{23}VV$ lineshape. The local contribution of the $O_{2s}O_{2p}$ band at ~54 eV now matches up more with the 50 eV peak in the experimental Auger lineshape of Fig. 1. The .4 relative intensity of this peak also is of the proper magnitude to account for the intensity under the experimental peak since the theoretical peak was way too small in the earlier work. The shoulder at 68 eV in the experimental lineshape we have previously suggested may be due to a shake satellite. It now appears it could be due to the local contribution of the $O_{2p}O_{2p}$ band at ~70 eV with a relative intensity of .7. The intensity of .7, somewhat less than the nearby 1.2 intensity of the contributions at 63 eV, seems qualitatively correct if it is to account for the 68 eV shoulder. The small local contribution of the $O_{2s}O_{2s}$ band at 37 eV falls under the Si L_1 L_{23} V peak which we examined earlier (1).

It appears that the local contribution is sufficiently removed in energy from the non-local contributions that they tend to fall under different experimental peaks and thus final state correlation effects are visible in the Si $L_{23}VV$ Auger lineshape. Although the energy alignment (both absolute and relative) is rather good, it does appear for both the O_{2s}-O_{2p} and O_{2p}-O_{2p} bands that the separation between the local and non-local contributions should be about 2 eV larger. This could easily be accounted for by somewhat larger values of the two center repulsion integrals $U(Si_{3p}, O_{2p})$.

3. Summary and Conclusion

In both the O KVV and the Si $L_{23}VV$ Auger lineshapes there is some evidence that the two center repulsion integrals u_{mn} should be larger. The "classical" approximation is the Mataga-Nishimoto (MN), eq. (13), but others have recently been suggested. In a recent study by Dewar and Thiel (35), the Klopman approximation (K) (36)

$$u_{mn} = e^2 \left[R_{mn}^2 + \left(\frac{2e^2}{u_n+u_m} \right) \right]^{-1/2} \qquad (45)$$

was compared with the MN approximation and analytically evaluated two center integrals. The K integrals were found to be in general agreement with the analytical integrals, the MN integrals generally too small. In the event that the two center overlaps are known, Huang (15) has proposed the approximation (H)

$$u_{mn} = S_{mn} \left(\frac{u_n+u_m}{2} \right) + (1-S_{mn}) \frac{e^2}{R_{mn}} \quad . \qquad (46)$$

Using the overlap integrals evaluated for SiO_2 by Gilbert et. al. (37), we obtain the values given in Table 4 along with the MN and K integrals.

All three approximations behave properly in the limits $R_{mn} \rightarrow 0$ and $R_{mn} \rightarrow \infty$. It is in the intermediate regions that the approximations differ. On the other hand, it has been argued (38,39) that the appropriate long-range repulsion should behave as $e^2/(kR_{mn})$ where "k" is the dielectric constant of the solid and accounts for the background electron density in solids. In

SiO_2 $k \approx 4$, which would significantly decrease the Coulomb repulsion. However, in the short range region of interest here (nearest neighbor), the macroscopic dielectric constant is probably not appropriate. The results in Table 4 indicate the MN integrals are smaller than the others in the short range region. Our interpretation of the experimental Auger lineshapes suggest the M or K approximations to be the more appropriate.

In summary, we have in this work elucidated the role of final state hole-hole correlation effects in Auger lineshapes. In the O KLL case, the Auger lineshape reveals a strong localization onto a single Si_2O cluster; indeed, it almost appears atomic-like. In the Si $L_{23}VV$ case, the Auger lineshape reveals significant contributions from both the *local* (*both holes on the same* Si_2O sub-cluster) and non-local (the two holes on neighboring Si_2O sub-clusters) configurations.

Perhaps most significant in this work is the use of the Auger lineshapes to obtain near quantitative information about the hole-hole repulsion magnitudes and bandwidths. In general, the absolute energies of the Auger transitions indicate the magnitude of the one-center integrals, the relative energies and intensities of the local and non-local contributions some information about the two center repulsion integrals and bandwidths. This suggests that the quantitative interpretation of Auger lineshapes might be a useful tool for obtaining important electronic structure information in other insulators and semiconductors and in chemisorbed systems.

References

1. D. E. Ramaker, J. S. Murday, N. H. Turner, G. Moore, M. G. Lagally, and J. Houston, Phys. Rev. B19, 5375 (1979).
2. D. E. Ramaker and J. S. Murday, J. Vac. Sci. Technol. 16, 510 (1979).
3. M. K. Bernett, J. S. Murday, and N. H. Turner, J. Electron. Spectrosc. Related Phenom. 12, 375 (1977).
4. P. J. Bassett, T. E. Gallon, M. Prutton, and J. A. D. Matthew, Surf. Sci. 33, 213 (1972).
5. B. Fischer, R. A. Pollak, T. H. DeStefano, and W. D. Grobman, Phys. Rev. B15, 3193 (1977).
6. H. H. Madden, D. M. Zehner, and J. R. Noonan, Phys. Rev. 17, 3074 (1978).
7. D. R. Jennison, Phys. Rev. B18, 6996 (1978).
8. E. Antonides, E. C. Janse, and G. A. Sawatzky, Phys. Rev. B15, 1669 (1977).
9. J. Hubbard, Proc. Roy. Soc. London, A276, 238 (1963).
10. P. W. Anderson, Phys. Rev. 109, 1492 (1958).
11. M. Cini, Solid State Commun. 20, 605 (1976); Phys. Rev. B17, 2788 (1978).
12. G. A. Sawatzky, Phys. Rev. Lett. 39, 504 (1977).
13. R. G. Parr, "Quantum Theory of Molecular Electronic Structures," (W. A. Benjamin, N.Y., 1963).
14. D. J. Chadi. R. B. Laughlin, and J. D. Joannopoulos, "The Physics of SiO_2 and its Interfaces," S. T. Pantelides, ed. (Pergamon Press, N.Y., 1978), p. 55.

15. C. Huang, J. A. Moriarty, and A. Sher, Phys. Rev. B12, 5395 (1975); Phys. Rev. B14, 2539 (1976).

16. B. I. Dunlap, P. Mills, and D. E. Ramaker, Manuscript in preparation.

17. K. Nishimoto and N. Mataga, Z. Physik Chem. 12, 335 (1957).

18. J. B. Mann, Los Alamos Scientific Laboratory Report No. LASL-3690, 1967 (unpublished).

19. S. T. Pantelides and W. A. Harrison, Phys. Rev. B13, 2667 (1976).

20. J. R. Chelikovsky and M. Schlüter, Phys. Rev. B15, 4020 (1977).

21. E. J. McGuire, Phys. Rev. 185, 1 (1969); Phys. Rev. 2, 273 (1970); Phys. Rev. 3, 1801 (1971); Phys. Rev. A3, 587 (1971); Sandia Laboratories Research Report SC-RR-710075, 1975.

22. W. N. Asaad, Nucl. Phys. 66, 494 (1965).

23. E. J. McGuire, Phys. Rev. A16, 2365 (1977).

24. R. W. G. Wyckoff, "Crystal Structures," (Interscience, N.Y., 1963), Vol. 1.

25. R. N. Nucho and A. Madhukar, "The Physics of SiO_2 and Its Interfaces," S. T. Pantelides, ed. (Pergamon Press, N.Y., 1978), p. 60.

26. L. Oleari, L. DiSipio, G. DeMichelis, Mol. Phys. 10, 97 (1966).

27. D. L. Griscom, J. Non-Crystall. Solids 24, 155 (1977).

28. I. P. Batra, "The Physics of SiO_2 and Its Interfaces," S. T. Pantelides, ed. (Pergamon Press, N.Y., 1978), p. 65.

29. T. H. DiStefano and D. E. Eastman, Phys. Rev. Lett. 27, 1560 (1971).

30. H. Ibach and J. E. Rowe, Phys. Rev. B10, 710 (1974).

31. C. Sénévaud, "The Physics of SiO_2 and Its Interfaces," S. T. Pantelides, ed. (Pergamon Press, N.Y., 1978), p. 75.

32. W. N. Assad and E. H. S. Burhop, Proc. Phys. Soc. London 72, 369 (1958).

33. V. O. Kostroun, M. H. Chen, and B. Crasemann, Phys. Rev. A3, 533 (1971).

34. B. W. Shore and D. H. Menzel, "Principles of Atomic Spectra," (Wiley, New York, 1968).

35. M. J. S. Dewar and W. Thiel, Theoret. Chim. Acta (Berl.) 46, 89 (1977).

36. G. Klopman, J. Am. Chem. Soc. 86, 4550 (1964).

37. T. L. Gilbert, W. J. Stevens, H. Schrenk, M. Yoshimine, and P. S. Bagus, Phys. Rev. B8, 5977 (1973).

38. C. Kittel, "Introduction to Solid State Physics," 4th ed. (Wiley, N.Y., 1971), p. 373.

39. N. F. Mott and E. A. Davis, "Electronic Processes in Non-crystalline Materials," (Clarendon Press, Oxford, 1971), p. 132.

40. D. J. Chadi and M. L. Cohen, Phys. Stat. Col. 68, 405 (1975).

41. K. Schmidtal, Surface Sci. 77, 523 (1978).

42. V. M. Bermudez and V. H. Ritz, Phys. Rev. 15,

TABLE I. Definition of Atomic Orbitals and Hamiltonian Matrix for Two Model Clusters

a. Bonding and Antibonding Bands: B_1-A_1-B_2-A_2-B_3

Atomic Orbitals: φ_{A_1}, φ_{A_2}

$$\varphi_{H1} = (h_{B_1}+h_{B_2})/\sqrt{2}, \quad \varphi_{H2} = (h_{B_1}-h_{B_2})/\sqrt{2}$$

Hamiltonian Matrix:

	$\lvert\varphi_{A1}\rangle$	$\lvert\varphi_{H1}\rangle$	$\lvert\varphi_{H2}\rangle$	$\lvert\varphi_{A2}\rangle$
$\langle\varphi_{A1}\rvert$	α_A	V	0	0
$\langle\varphi_{H1}\rvert$	V	α_H	Γ	0
$\langle\varphi_{H2}\rvert$	0	Γ	α_H	V
$\langle\varphi_{A2}\rvert$	0	0	V	α_A

b. Non-bonding Bands on A: A_1-B_1-A_2-B_2-A_3-B_3-A_4

Atomic Orbitals: φ_{A_1}, φ_{A_2}, φ_{A_3}, φ_{A_4}

Hamiltonian Matrix:

	$\lvert\varphi_{A_1}\rangle$	$\lvert\varphi_{A_2}\rangle$	$\lvert\varphi_{A_3}\rangle$	$\lvert\varphi_{A_1}\rangle$
$\langle\varphi_{A_1}\rvert$	α_A	Γ	0	0
$\langle\varphi_{A_2}\rvert$	Γ	α_A	Γ	0
$\langle\varphi_{A_3}\rvert$	0	Γ	α_A	Γ
$\langle\varphi_{A_4}\rvert$	0	0	Γ	α_A

TABLE 2. Summary of Matrix Elements (tight binding parameters) obtained in this work and comparison with other reported results.

Matrix Element	This work (eV)	Tight Binding Calc. (eV) Chadi et al[14]	Nucho et al[25]
$\alpha(Si_h)$	-3 (-4)[a]	-4.6[b,c]	-7.9[b]
$\alpha(O_{2s})$	24	19.1[b]	
$\alpha(O_{2p})$	6 (5,8)[a]	6.3[b]	6.0[b]
$v(O_{2s},O_{2s})$	0	.15	
$v(O_{2p},O_{2p})$	1	.45	
$v(Si_h, Si_h)$	2[d]	1.6[e]	
$v(Si_h, O_{2s})$	5	6.2[e]	
$v(Si_h,O_{2p})$	6[d]	5.4[e]	5, 2[f]
$u(O_{2s})$	15[g]		
$u(O_{2p})$	15[g]		
$u(Si_h)$	11,[g,h]		

[a]Values in parentheses were used for the Si_4O_5 cluster where $\alpha(O_{2p}(b))$ and $\alpha(O_{2p}(nb))$ were allowed to be different, i.e., 5 and 8, respectively.

[b]4.5 eV added to literature values to change zero point energy from the top of the valence band to the Fermi level (1).

[c]$\alpha(Si_h) = (\alpha(Si_{3s}) + 3\alpha(Si_{3p}))/4$ for sp^3 hybrid (40). Values of $\alpha(Si_{3s})$ and $\alpha(Si_{3p})$ from ref. 14.

(continued)

(Table 2, continued)

[d] In the Si_4O_3 cluster calculations, a linear combination of the sp^3 hybrids h_i were utilized, i.e., $H = \frac{1}{\sqrt{2}}(h_1 \pm h_2)$. Thus $V(Si_H, Si_H) = 1/2\ V(Si_h, Si_h) = 1$ and $V(Si_H, O_{2p}) = \sqrt{2}V(Si_h, O_{2p}) = 9$.

[e] $V(Si_h, Si_h) = 1/4(\alpha(Si_{3s}) - \alpha(Si_{3p}))$ (40).
$V(Si_h, O_{2s/p}) = 1/2[V(Si_{3s}, O_{2s/p_\sigma}) + V(Si_{3p_\sigma}, O_{2s/p_\sigma})]$
where by summetry $V(Si_{3p_\Pi}, O_{2s/p_\sigma}) = 0$.

[f] Two different sets of parameters were reported, the values depending upon the region of the DOS fitted (25).

[g] u was treated throughout as a parameter in the calculations to gradually turn on the effects of correlation. However, our best estimates are given here as determined from Manns (18) integral tables and estimates of the correlation or static relaxation contributions (1).

[h] $u(Si_H) = 1/2[u(Si_{h1}) + u(Si_{h1}, Si_{h2})] = 7$.

TABLE 4 - Probabilities P_{ij} for hole occupancy on the i^{th} and j^{th} O atoms in the 2p nonbonding band of an O_7 cluster in SiO_2

Peak[1]	u	Energy of State in Band	Same Center		Nearest Neighbor		2nd and 3rd Neighbors, etc.
			P_{11}[2]	$\Sigma_{i\neq 1} P_{ii}$	$\Sigma_{i\neq 1} P_{1i}$	$\Sigma^{(3)}_{i\neq j\neq 1} P_{ij}$	$\Sigma^{(4)}_{i\neq j\neq 1} P_{ij}$
	0	-3.29	.475	.016	.429	.032	.048
1	5	.20	.275	.018	.528	.092	.104
	8	1.31	.151	.000	.563	.138	.148
	15	2.54	.043	.000	.556	.177	.224
	0	-2.00	0	.435	.000	.390	.176
2	5	2.06	.019	.502	.013	.460	.006
	8	3.74	.024	.322	.037	.577	.039
	15	5.60	.003	.074	.024	.678	.222
	0	2.00	.429	.071	.143	.143	.214
3	5	5.51	.399	.007	.009	.044	.581
	8	6.63	.216	.020	.034	.001	.730
	15	8.16	.072	.043	.281	.056	.547
	0	4.00	0	.167	0	.333	.500
4	5	7.01	.139	.342	.468	.274	.197
	8	9.19	.357	.432	.042	.143	.027
	15	15.55	.447	.505	.011	.037	.001
	0	7.29	.096	.079	.429	.158	.237
5	5	10.38	.166	.147	.401	.170	.116
	8	11.93	.251	.226	.324	.142	.057
	15	16.87	.435	.379	.127	.052	.007

[1] Peak numbers correspond to those in Figure 4.

[2] Atom 1 is the atom with the initial core hole.

[3] Only P_{ij} terms in which i and j are nearest neighbors are included.

[4] Only P_{ij} terms in which i and j are not nearest neighbors are included.

TABLE 4

The Auger Transition Rates After CI Mixing of the Terms Coming from the Tetrahedral Si_5O_4 Cluster

Molecular Term*		Transition Rate
O_{2s}-O_{2s} or O_{2p}-O_{2p} terms	$^1A_1$ (2)	$[\, D(a_1^2,\ ^1A_1)c_s^2(a_1)M_{css}(^1S)$
		$+D(t_2^2,\ ^1A_1)c_p^2(t_2)M_{cpp}(^1S)\,]^2$
	$^1T_2$ (2)	$[\, D(a_1t_2,\ ^1T_2)c_s(a_1)c_p(a_1)M_{csp}(^1P)$
		$+D(t_2^2,\ ^1T_2)c_p^{\,2}(t_2)(.6)M_{cpp}(^1D)\,]^2$
	$^3T_2$	$[\, c_s(a_1)c_p(a_1)M_{csp}(^3P)\,]^2$
	$^3T_1$	$[\, c_p^2(t_1)M_{cpp}(^3P)\,]^2$
	^1E	$[\, c_p^2(t_2)(.4)M_{cpp}(^1D)\,]^2$
O_{2s}-O_{2p} terms	$^{1/3}A_1$ (4)	$[\, D(a_1a_1',\ ^{1/3}A_1)c_s(a_1)c_s(a')M_{css}(^{1/3}S)$
		$+D(t_2t_2',\ ^{1/3}A_1)c_p(t_2)c_p(t_2')M_{cpp}(^{1/3}S)\,]^2$
	$^{1/3}T_2$ (6)	$[\, D(a_1t_2',\ ^{1/3}T_2)c_s(a_1)c_p(t_2')M_{csp}(^{1/3}P)$
		$+D(a_1't_2,\ ^{1/3}T_2)c_s(a_1')c_p(t_2)M_{csp}(^{1/3}P)$
		$+D(t_2't_2,\ ^{1/3}T_2)c_p(t_2)c_p(t_2')(.6)M_{cpp}(^{1/3}D)\,]^2$
	$^{1/3}E$	$[\, c_p(t_2)c_p(t_2')(.4)M_{cpp}(^{1/3}D)\,]^2$
	$^{1/3}T_1$	$[\, c_p(t_2)c_p(t_2')M_{cpp}(^{1/3}P)\,]^2$

*Number in parentheses indicates number of states having this symmetry.

TABLE 5. Comparison of Approximations for the Two-Center Coulomb Repulsion Integrals in SiO_2[1]

Item	Si-O	O-O	Si-Si
R_{mn} (Å)	1.5	2.5	3.0
Overlap $\langle\varphi_m/\varphi_n\rangle$[2]	0.26	0.063	0.33
Mataga-Nishimoto[17] u_{mn} (eV)	5.5	4.1	3.3
Klopman[36] u_{mn} (eV)	7.7	5.3	4.4
Huang[15] u_{mn} (eV)	10.4	6.3	6.8

[1]The assumed values of $u(Si_{3p})$ and $u(O_{2p})$ were 11 and 15 eV, respectively.

[2]From Gilbert et.al. (37).

Figure Captions

Fig. 1. (a) A comparison of the experimental (solid line) O KVV Auger lineshape with the theoretical lineshape determined previously (1). (b) The difference between the experimental and calculated lineshapes. The peaks at 475 and 495 eV have been identified to be shake satellites. The peak at 511 eV is the subject of this work. (c) A comparison of the experimental (solid line) Si $L_{23}VV$ Auger lineshape with the theoretical lineshape determined previously (1). (d) The difference between the experimental and calculated lineshapes. The peaks at 52 and 70 eV have been attributed to shake satellites, but in this work are shown also to arise partially from correlation effects. Possible sources of the peak at 84 eV are summarized elsewhere (1,27,41,42).

Fig. 2. Auger energies and relative intensities of the eigenvalues arising from an LCAO-MO-CI calculation on the Si_4O_3 cluster for various values of u_O and u_{Si}. Contributions from the $O_{2p}(b)$-$O_{2p}(b)$, $O_{2p}(nb)$-$O_{2p}(b)$ and $O_{2p}(nb)$-$O_{2p}(nb)$ bands are indicated by the light solid, open, and heavy solid lines, respectively. Contributions involving the O_{2s} band are ignored here. Numbers indicate the intensity in arbitrary units.

Fig. 3. Column one contains the one-electron $O_{2p}(nb)$ local density of states on the central O atom arising from an LCAO-MO calculation on an O_{16} cluster. Columns two through four contain the relative $O_{2p}(nb)$-$O_{2p}(nb)$ Auger energies and intensities of the eigenvalues arising from a CI calculation on the O_{16} cluster for various values of one- and two-center hole-hole repulsion integrals u_1 and u_{12}. The total intensity has been normalized to 100. The local DOS energies are equal to 16 eV minus the energies indicated; the Auger energies are equal to 517 eV minus the energies indicated. The peak numbers refer to Table 3. The $O_{2p}(nb)$ bandwidth as exhibited in column one is ~6 eV.

Fig. 4. Comparison of results for the $O_{2p}(nb)$-$O_{2p}(nb)$ Auger lineshape. On the lower left is plotted the percent non-local intensity of the total Auger intensity vs. u/Γ. On the upper right is plotted the difference in energy between the centroids of the local and non-local Auger contributions vs. u/Γ. u is the one-center hole-hole repulsion energy parameter; Γ is the $O_{2p}(nb)$ bandwidth as determined from the spread of the one-electron DOS of the corresponding n cluster. Results are shown for clusters containing three atoms (dotted line), seven atoms (dashed line), 16 atoms with $u_{ij} = 0$ (dot-dashed line), and 16 atoms with $u_{ij} \neq 0$ (solid line).

Fig. 5. Comparison of results for the Si $L_{23}VV$ Auger lineshape. In column one are the Auger energies and relative intensities resulting from the fold of the one-electron DOS local to the central Si atom as determined from a LCAO-MO calculation on an Si_5O_4 cluster. The position of the final state holes is indicated at the far left in terms of the M.O.'s as named in tetrahedral symmetry. The symbols (s, p) in parentheses indicate the dominant central Si atom contribution. In column two, hole-hole repulsion is included without CI mixing for u_{Si} = 10 and u_O = 15 eV. The third column gives results with CI mixing. The terms $^{2S+1}$ (A, E, or T) are given as determined by group theory in T_d symmetry; the dominant configuration mixing given in parentheses after the term symbol. Numbers given indicate intensities in arbitrary units.

Acknowledgement: The author wishes to thank the Surface Chemistry Branch of the Naval Research Laboratory for its assistance in the preparation of this manuscript and for valuable discussions with several members of the branch.

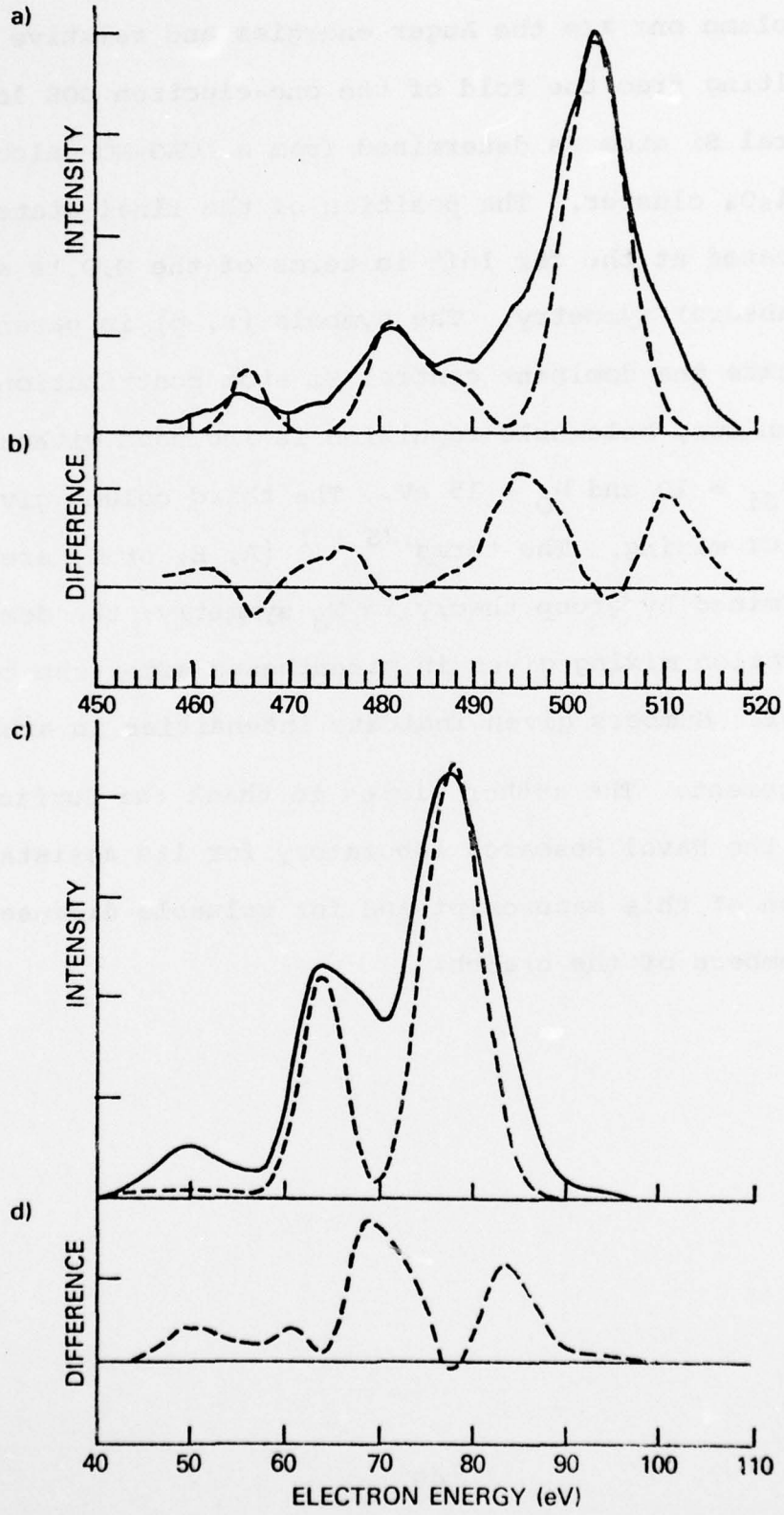
a)
INTENSITY
b)
DIFFERENCE
450
460
470
480
490
500
510
520
c)
INTENSITY
d)
DIFFERENCE
40
50
60
70
80
90
100
110
ELECTRON ENERGY (eV)

FIG. 1

$u_o(u_{Si}) = 0(0)$
5(2) eV
15(7) eV
AUGER ENERGY (eV)
520
518
516
514
512
510
508
506
504
502
500
100
200
35
38
100
35
14
38
26
12
34
55
5
28
133
.6
177
32
5
78
16
31
3
10
4
.6
.4
20
133
120
254
52

FIG. 2

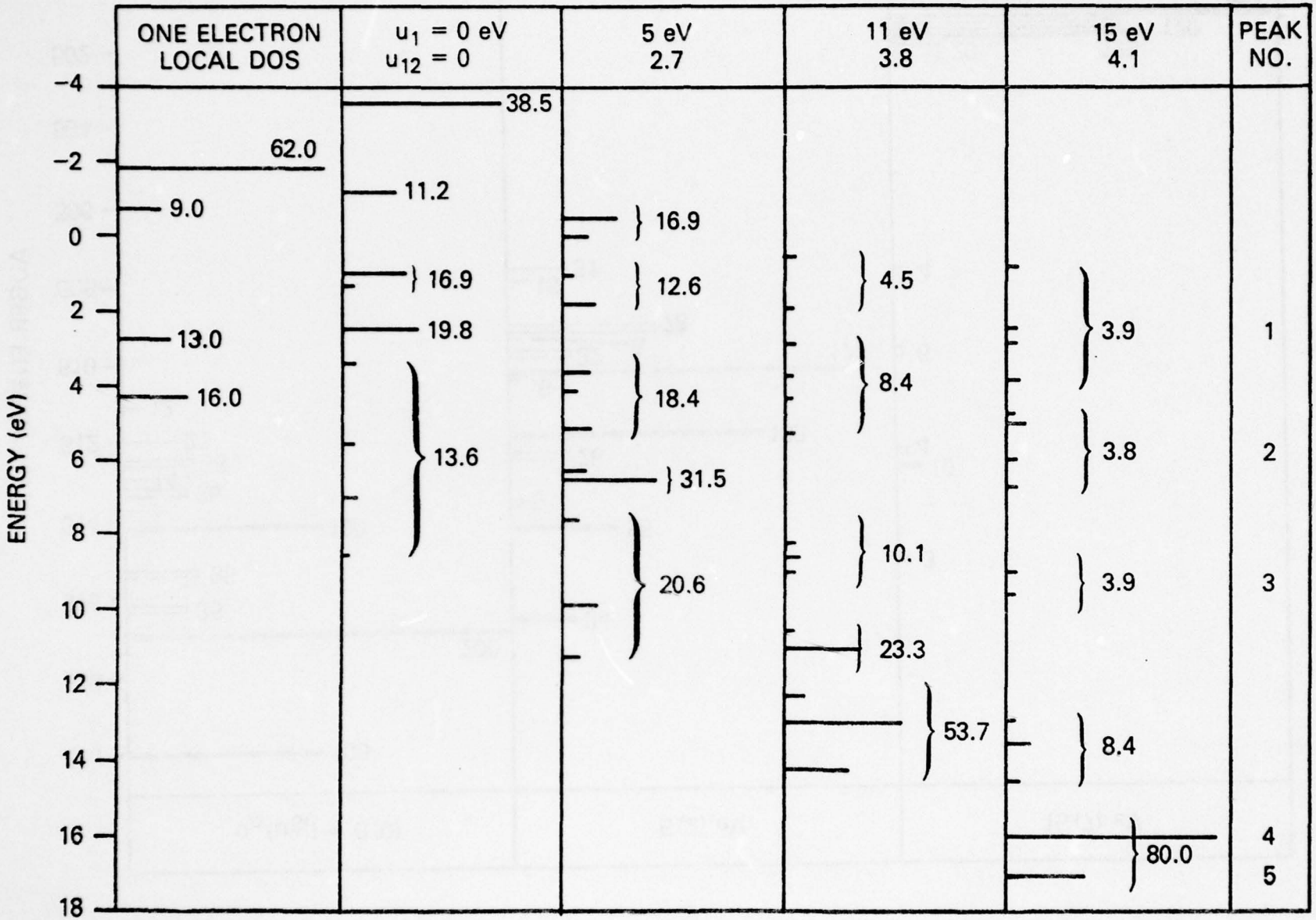
ONE ELECTRON LOCAL DOS
u_1 = 0 eV
u_{12} = 0
5 eV
2.7
11 eV
3.8
15 eV
4.1
PEAK NO.
ENERGY (eV)
−4
−2
0
2
4
6
8
10
12
14
16
18
62.0
9.0
13.0
16.0
38.5
11.2
16.9
19.8
13.6
16.9
12.6
18.4
31.5
20.6
4.5
8.4
10.1
23.3
53.7
3.9
3.8
3.9
8.4
80.0
1
2
3
4
5

FIG. 3

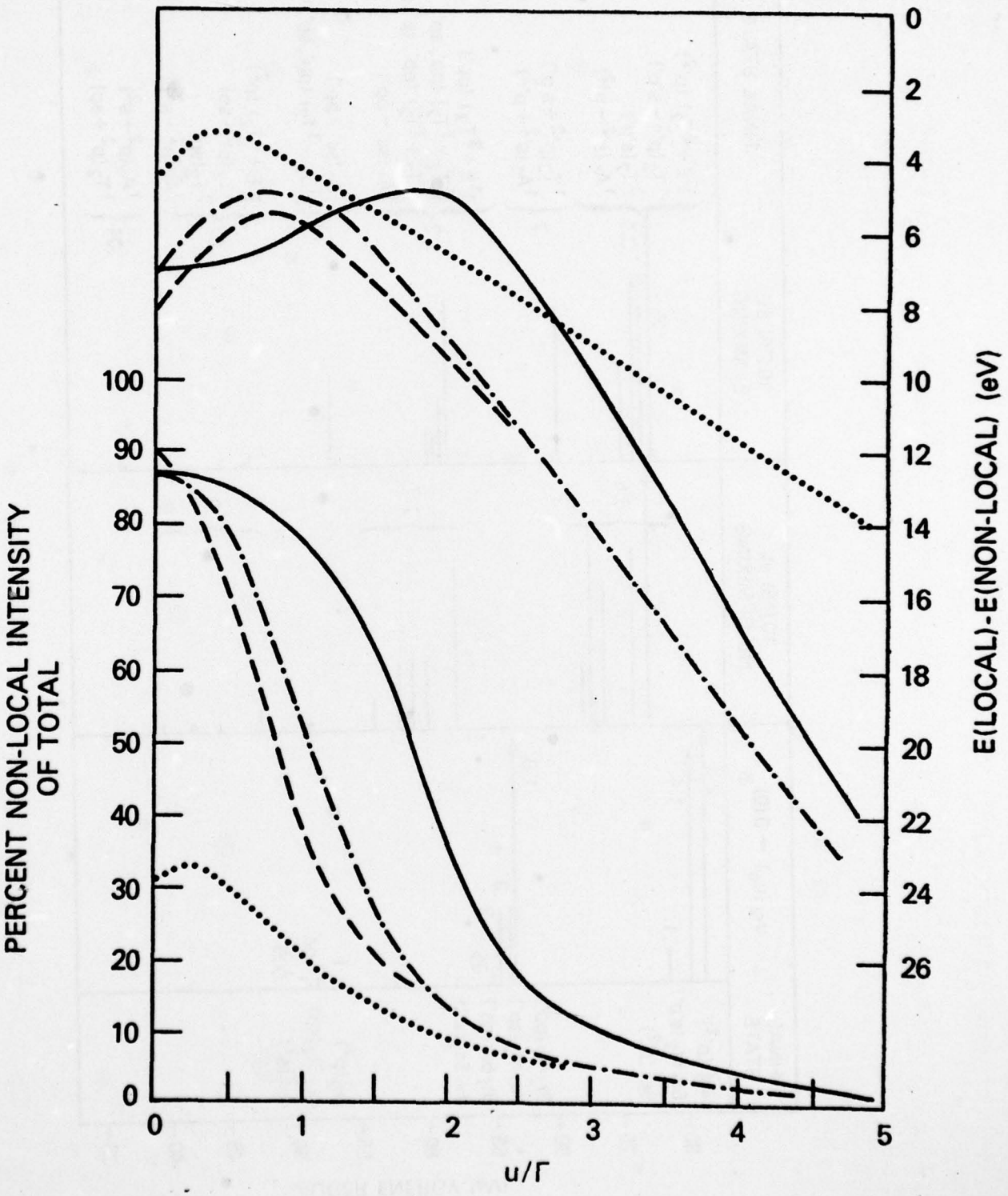
PERCENT NON-LOCAL INTENSITY OF TOTAL
100
90
80
70
60
50
40
30
20
10
0
0
1
2
3
4
5
u/Γ
E(LOCAL)-E(NON-LOCAL) (eV)
0
2
4
6
8
10
12
14
16
18
20
22
24
26

FIG. 4

FIG. 5

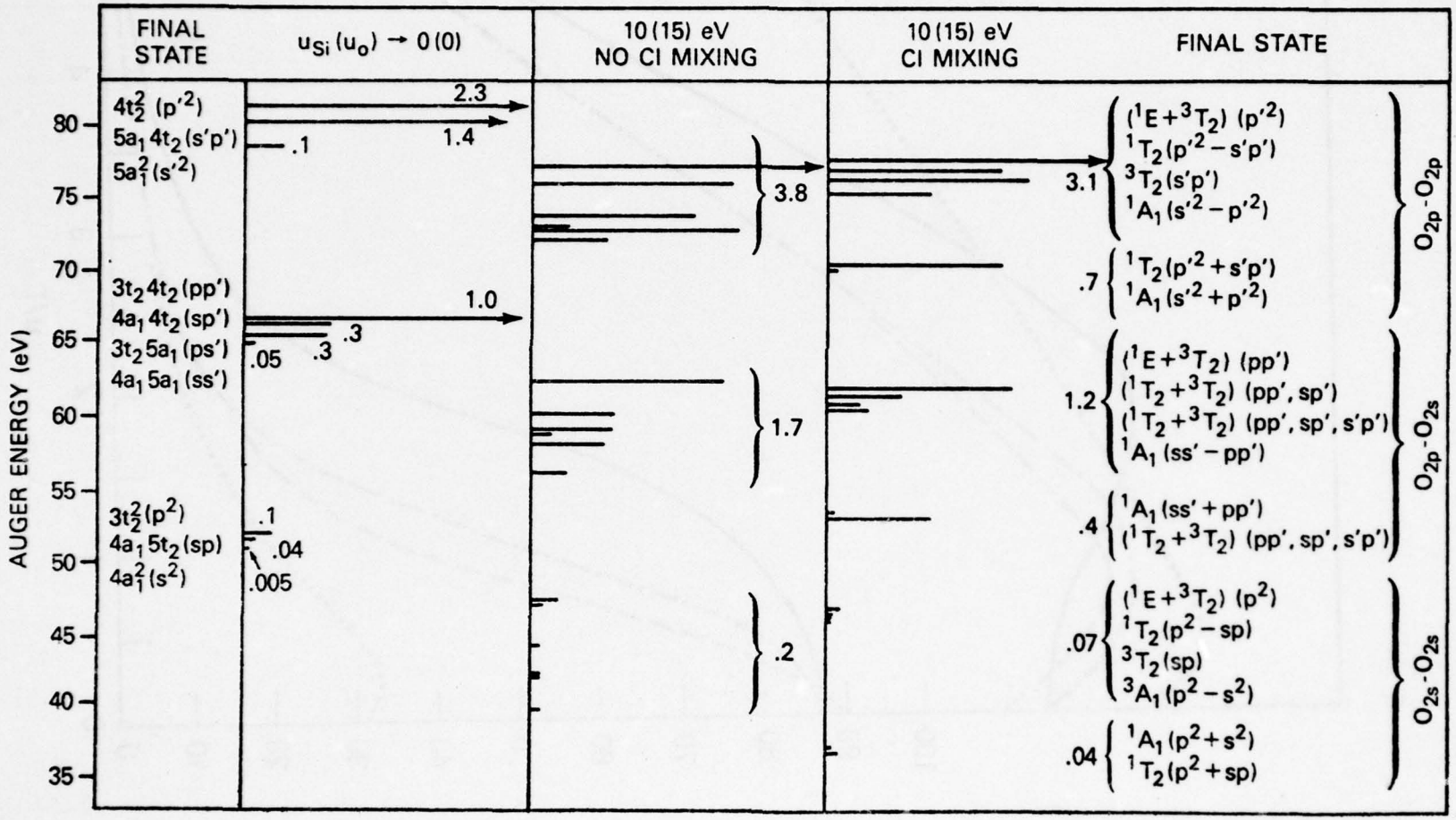
FINAL STATE
$u_{Si}(u_o) \rightarrow 0(0)$
10(15) eV NO CI MIXING
10(15) eV CI MIXING
FINAL STATE
AUGER ENERGY (eV)
80
75
70
65
60
55
50
45
40
35
$4t_2^2(p'^2)$
$5a_1 4t_2(s'p')$
$5a_1^2(s'^2)$
$3t_2 4t_2(pp')$
$4a_1 4t_2(sp')$
$3t_2 5a_1(ps')$
$4a_1 5a_1(ss')$
$3t_2^2(p^2)$
$4a_1 5t_2(sp)$
$4a_1^2(s^2)$
2.3
1.4
.1
1.0
.3
.05
.3
.1
.04
.005
3.8
1.7
.2
3.1
$({}^1E + {}^3T_2)(p'^2)$
${}^1T_2(p'^2 - s'p')$
${}^3T_2(s'p')$
${}^1A_1(s'^2 - p'^2)$
.7
${}^1T_2(p'^2 + s'p')$
${}^1A_1(s'^2 + p'^2)$
1.2
$({}^1E + {}^3T_2)(pp')$
$({}^1T_2 + {}^3T_2)(pp', sp')$
$({}^1T_2 + {}^3T_2)(pp', sp', s'p')$
${}^1A_1(ss' - pp')$
.4
${}^1A_1(ss' + pp')$
$({}^1T_2 + {}^3T_2)(pp', sp', s'p')$
.07
$({}^1E + {}^3T_2)(p^2)$
${}^1T_2(p^2 - sp)$
${}^3T_2(sp)$
${}^3A_1(p^2 - s^2)$
.04
${}^1A_1(p^2 + s^2)$
${}^1T_2(p^2 + sp)$
O_{2p}-O_{2p}
O_{2p}-O_{2s}
O_{2s}-O_{2s}

P4-2/A23

472:GAN:716:tam
78u472-608

TECHNICAL REPORT DISTRIBUTION LIST, GEN

	No. Copies
Office of Naval Research Attn: Code 472 800 North Quincy Street Arlington, Virginia 22217	2
ONR Branch Office Attn: Dr. George Sandoz 536 S. Clark Street Chicago, Illinois 60605	1
ONR Branch Office Attn: Scientific Dept. 715 Broadway New York, New York 10003	1
ONR Branch Office 1030 East Green Street Pasadena, California 91106	1
ONR Branch Office Attn: Dr. L. H. Peebles Building 114, Section D 666 Summer Street Boston, Massachusetts 02210	1
Director, Naval Research Laboratory Attn: Code 6100 Washington, D.C. 20390	1
The Assistant Secretary of the Navy (R,E&S) Department of the Navy Room 4E736, Pentagon Washington, D.C. 20350	1
Commander, Naval Air Systems Command Attn: Code 310C (H. Rosenwasser) Department of the Navy Washington, D.C. 20360	1
Defense Documentation Center Building 5, Cameron Station Alexandria, Virginia 22314	12
Dr. Fred Saalfeld Chemistry Division Naval Research Laboratory Washington, D.C. 20375	1
U.S. Army Research Office Attn: CRD-AA-IP P.O. Box 1211 Research Triangle Park, N.C. 27709	1
Naval Ocean Systems Center Attn: Mr. Joe McCartney San Diego, California 92152	1
Naval Weapons Center Attn: Dr. A. B. Amster, Chemistry Division China Lake, California 93555	1
Naval Civil Engineering Laboratory Attn: Dr. R. W. Drisko Port Hueneme, California 93401	1
Department of Physics & Chemistry Naval Postgraduate School Monterey, California 93940	1
Dr. A. L. Slafkosky Scientific Advisor Commandant of the Marine Corps (Code RD-1) Washington, D.C. 20380	1
Office of Naval Research Attn: Dr. Richard S. Miller 800 N. Quincy Street Arlington, Virginia 22217	1
Naval Ship Research and Development Center Attn: Dr. G. Bosmajian, Applied Chemistry Division Annapolis, Maryland 21401	1
Naval Ocean Systems Center Attn: Dr. S. Yamamoto, Marine Sciences Division San Diego, California 91232	1
Mr. John Boyle Materials Branch Naval Ship Engineering Center Philadelphia, Pennsylvania 19112	1

TECHNICAL REPORT DISTRIBUTION LIST, GEN

	No. Copies
Dr. Rudolph J. Marcus Office of Naval Research Scientific Liaison Group American Embassy APO San Francisco 96503	1
Mr. James Kelley DTNSRDC Code 2803 Annapolis, Maryland 21402	1

P4-2/B5

472:GAN:716:tam
78u472-608

TECHNICAL REPORT DISTRIBUTION LIST, 056

	No. Copies
Dr. D. A. Vroom IRT P.O. Box 80817 San Diego, California 92138	1
Dr. G. A. Somorjai Department of Chemistry University of California Berkeley, California 94720	1
Dr. L. N. Jarvis Surface Chemistry Division 4555 Overlook Avenue, S.W. Washington, D.C. 20375	1
Dr. J. B. Hudson Materials Division Rensselaer Polytechnic Institute Troy, New York 12181	1
Dr. John T. Yates Surface Chemistry Section National Bureau of Standards Department of Commerce Washington, D.C. 20234	1
Dr. Theodore E. Madey Surface Chemistry Section Department of Commerce National Bureau of Standards Washington, D.C. 20234	1
Dr. J. M. White Department of Chemistry University of Texas Austin, Texas 78712	1
Dr. Keith H. Johnson Department of Metallurgy and Materials Science Massachusetts Institute of Technology Cambridge, Massachusetts 02139	1
Dr. J. E. Demuth IBM Corportion Thomas J. Watson Research Center P.O. Box 218 Yorktown Heights, New York 10598	1
Dr. C. P. Flynn Department of Physics University of Illinois Urbana, Illinois 61801	1
Dr. W. Kohn Department of Physics University of California (San Diego) LaJolla, California 92037	1
Dr. R. L. Park Director, Center of Materials Research University of Maryland College Park, Maryland 20742	1
Dr. W. T. Peria Electrical Engineering Department University of Minnesota Minneapolis, Minnesota 55455	1
Dr. Narkis Tzoar City University of New York Convent Avenue at 138th Street New York, New York 10031	1
Dr. Chia-wei Woo Department of Physics Northwestern University Evanston, Illinois 60201	1
Dr. D. C. Mattis Polytechnic Institute of New York 333 Jay Street Brooklyn, New York 11201	1
Dr. Robert M. Hexter Department of Chemistry University of Minnesota Minneapolis, Minnesota 55455	1
Dr. R. P. Van Duyne Chemistry Department Northwestern University Evanston, Illinois 60201	1

TECHNICAL REPORT DISTRIBUTION LIST, 056

	No. Copies
Dr. Leonard Wharton Department of Chemistry James Franck Institute 5640 Ellis Avenue Chicago, Illinois 60637	1
Dr. M. G. Lagally Department of Metallurgical and Mining Engineering University of Wisconsin Madison, Wisconsin 53706	1
Dr. Robert Gomer Department of Chemistry James Franck Institute 5640 Ellis Avenue Chicago, Illinois 60637	1
Dr. R. G. Wallis Department of Physics University of California, Irvine Irvine, California 92664	1
Dr. D. Ramaker Chemistry Department George Washington University Washington, D.C. 20052	1
Dr. P. Hansma Chemistry Department University of California, Santa Barbara Santa Barbara, California 93106	1
Dr. P. Hendra Chemistry Department Southhampton University England S09JNH	1
Professor P. Skell Chemistry Department Pennsylvania State University University Park, Pennsylvania 16802	1
Dr. J. C. Hemminger Chemistry Department University of California, Irvine Irvine, California 92717	1
Dr. Martin Fleischmann Department of Chemistry Southampton University Southampton 509 5NH Hampshire, England	1
Dr. J. Osteryoung Chemistry Department State University of New York at Buffalo Buffalo, New York 14214	1
Dr. G. Rubloff I.B.M. Thomas J. Watson Research Center P. O. Box 218 Yorktown Heights, New York 10598	1
Dr. J. A. Gardner Department of Physics Oregon State University Corvallis, Oregon 97331	1
Dr. G. D. Stein Mechanical Engineering Department Northwestern University Evanston, Illinois 60201	1
Dr. K. G. Spears Chemistry Department Northwestern University Evanston, Illinois 60201	1
Dr. R. W. Plummer University of Pennsylvania Department of Physics Philadelphia, Pennsylvania 19104	1
Dr. E. Yeager Department of Chemistry Case Western Reserve University Cleveland, Ohio 41106	2